

Revisiting the Classics: On the Statistics of Dust Formation in Novae

Atticus Chong^{1*}, Elias Aydi^{2,1†}, Peter Craig¹, Laura Chomiuk¹, Ashley Stone³, Jay Strader¹, Adam Kawash¹, Kirill V. Sokolovsky⁴, and Fred Walter⁵

¹Center for Data Intensive and Time Domain Astronomy, Department of Physics and Astronomy, Michigan State University, East Lansing, MI 48824, USA

²Department of Physics & Astronomy, Texas Tech University, Box 41051, Lubbock, TX, 79409-1051, USA

³Department of Physics & Astronomy, West Virginia University, White Hall, Morgantown, 26501-6315, WV, USA

⁴Department of Astronomy, University of Illinois at Urbana-Champaign, 1002 W. Green Street, Urbana, IL 61801, USA

⁵Department of Physics & Astronomy, Stony Brook University, Stony Brook, NY 11794-2100

ABSTRACT

While nova eruptions produce some of the most common and dramatic dust formation episodes among astrophysical transients, the demographics of dust-forming novae remain poorly understood. Here, we present a statistical study of dust formation in 40 novae with high-quality optical/IR light curves, quantitatively distinguishing dust-forming from non-dust-forming novae while exploring the properties of the dust events. We find that 50–70 % of novae produce dust, significantly higher than previous estimates. Dust-forming novae can be separated from those that do not show dust formation by using the largest redward ($V - K$) colour change from peak visible brightness; ($V - J$) or ($V - H$) offer useful but less sensitive constraints. This makes optical+IR photometry a powerful tool to quantify dust formation in novae. We find that novae detected in GeV γ -rays by *Fermi*-LAT appear to form dust more often than novae not detected by *Fermi*, implying a possible connection between γ -ray producing shocks and dust production. We also find that novae that evolve very quickly ($t_2 < 10$ days) are much less likely to form dust, in agreement with previous findings. We confirm a correlation between t_2 and the time of the onset of dust formation (which occurs ~ 1 week–3 months after maximum light), but conclude that it is primarily an observational artifact driven by dust formation determining when a nova drops 2 mag below peak. The significant fraction of novae that form dust make them ideal laboratories in our Galactic backyard to tackle the puzzle of dust formation around explosive transients.

Key words: stars: novae, cataclysmic variables — white dwarfs — dust, extinction.

1 INTRODUCTION

A classical nova eruption is a transient event driven by a thermonuclear runaway on the surface of an accreting white dwarf in a close binary system (see Bode & Evans 2008; Della Valle & Izzo 2020; Chomiuk et al. 2021a for recent reviews). The thermonuclear runaway leads to the ejection of at least part of the accreted envelope ($10^{-7} - 10^{-3} M_{\odot}$) with velocities ranging between 200 and 10,000 km s⁻¹ (Payne-Gaposchkin 1957; Gallagher & Starrfield 1978; Yaron et al. 2005; Aydi et al. 2020b). 25–50 nova eruptions are expected each year in our Milky Way Galaxy, with around half of them actually being discovered by optical and infrared (IR) surveys (De et al. 2021; Kawash et al. 2022; Zuckerman et al. 2023). Nova eruptions can recur on a given white dwarf, sometimes with recurrence times as short as a year (e.g., Darnley & Henze 2020), but usually with recurrence times longer than human timescales, setting the observational distinction between ‘classical’ novae (with a single observed eruption) and

‘recurrent’ novae (with multiple eruptions in recorded history; Schaefer 2010; Darnley 2021).

After the nova, nuclear burning can be sustained on the white dwarf surface for days–years, which manifests as a super-soft X-ray source (Schwarz et al. 2011; Wolf et al. 2013; Page et al. 2020). Emission from the nuclear-burning white dwarf photo-ionizes the nova ejecta, and the ionization front moves outward in the ejecta with time (e.g. Beck et al. 1990; Williams 1990); once ionized, the ejecta are expected to be sustained at a temperature around 10^4 K (Cunningham et al. 2015). In addition, shocks within the ejecta can further heat portions of the ejecta up to X-ray emitting temperatures (Mukai et al. 2008; Metzger et al. 2015; Aydi et al. 2020a; Gordon et al. 2021).

Despite these warm-to-hot temperatures expected and observed in nova ejecta, somehow nova eruptions find a way to form dust. A dust formation event in a nova light curve typically presents as a dip in the optical light curve and/or a rise in the IR brightness, as the dust absorbs optical radiation and then re-emits it mostly in the IR (Gehrz 2008; Strope et al. 2010). The ‘dust dip’ in the optical light curve is usually followed by a recovery, caused by the dispersion or destruction of the dust, to a level fainter than that at the

* E-mail: chongatt@msu.edu, oh0sitm@gmail.com

† E-mail: eaydi@ttu.edu

start of the dip (Strope et al. 2010). This evolution of the visible and IR brightness is demonstrated in data from as early as 1976 (e.g., NQ Vul; Ney & Hatfield 1978).

These signatures of dust formation in novae have been observed for over 50 years (Geisel et al. 1970), and have been reviewed by Gehrz (1988, 2002, 2008); Gehrz et al. (1998); Evans (1990, 1997, 2001); Evans & Rawlings (2008); Evans & Gehrz (2012), and Banerjee & Ashok (2012). Dust formation usually occurs between one and five months post-eruption (Williams et al. 2013), with some rare exceptions where dust forms on timescales that are significantly shorter (e.g., V745 Sco; Banerjee et al. 2023b) or longer (e.g., the unique He nova V445 Pup; Woudt et al. 2009). The dust grains in novae are usually carbon-rich (and indeed, dust formation episodes are most commonly hosted by carbon-oxygen white dwarfs), but in some cases they are silicate-rich (Gehrz et al. 1998). Typical dust masses produced in novae reach $10^{-8} - 10^{-6} M_{\odot}$, comprising 0.001–10 per cent of the ejecta mass (Gehrz et al. 1998; Gehrz 2008), but not all novae form dust. While it is clear that much of the newly formed dust is subsequently destroyed, primarily from irradiation by the supersoft X-ray source (Evans et al. 2017; Gehrz et al. 2018), in at least some novae there is evidence that some dust can survive to late times (e.g. José & Hernanz 2007; Evans et al. 2010; Banerjee et al. 2018).

The formation of dust in explosive transients remains a major outstanding mystery, and novae are no exception. It is unclear exactly where and how dust forms in the nova ejecta, given that they are warm, rapidly expanding, dropping in density, and irradiated by energetic emission. Early models of dust formation pointed out that nova nucleation sites must be neutral and shielded from the hard emission of the supersoft X-ray source (Gallagher 1977; Rawlings 1988; Rawlings & Williams 1989). There has long been evidence for dense structures or clumps in nova ejecta (e.g. Gallagher & Anderson 1976; Williams 1994; O’Brien & Bode 2008), and it has been hypothesized that dust forms in these overdensities (Rawlings 1988). In light of the recent discovery of GeV γ -rays and strong energetic shocks associated with nova eruptions (Abdo et al. 2010; Ackermann et al. 2014; Metzger et al. 2014, 2015), a novel origin of nova dust has been suggested: that dust forms in radiative shock fronts internal to the nova ejecta (Derdzinski et al. 2017). This theory predicts that the rapidly-cooling, high-density, shocked gas could create the ideal environment for dust to condensate, while shielding it from the irradiation of the central white dwarf (Derdzinski et al. 2017). This theory is supported by recent observations of radio synchrotron flares—associated with particle acceleration in shocks—contemporaneous with dust dips in the optical (Chomiuk et al. 2021b; Babul et al. 2022). Shocks are seen as the primary sites of dust formation in massive-star colliding-wind binaries (Usov 1991; Lau et al. 2022), bolstering the case that the same shocks that produce γ -rays in novae may also form dust.

Their nearby distances and \sim Eddington luminosities make novae the brightest IR transients regularly detected in the sky, and dust formation keeps them bright at IR wavelengths, often for months. This makes novae one of the best laboratories to observe and explore dust formation around explosive transients. As we will see in this paper, novae regularly reach K -magnitudes < 8 , and the brightest novae saturated our IR detector on the SMARTS 1.3m telescope ($K < 5$). Wide-field

time-domain IR surveys are currently coming of age, with Y , J , and H -band surveys like Gattini-IR (De et al. 2020, 2021), WINTER (Lourie et al. 2020), and PRIME (Yama et al. 2023; Hamada et al. 2024). These surveys will be routinely detecting novae and producing high-quality IR light curves. However, most wide-field surveys are only observing in a single IR band, and it is currently unclear how well one can determine if a nova formed dust from these single-band data alone, or in combination with optical monitoring. This paper seeks to clarify what we can expect from these time-domain surveys, and how we can use them to tell if a nova has formed dust.

With a new hypothesis that dust is formed in nova shocks, and a new generation of IR time-domain surveys, we here revisit the pioneering studies discussed above with a more modern, larger dataset in order to (1) provide an up-to-date estimate of the percentage of novae that produce dust, (2) explore the properties of the dust forming novae, and (3) present a simple, easy-to-measure diagnostic of dust formation in novae, with the aim of motivating future observations and surveys in the near/mid-IR wavelengths. The observations and sample selection is presented in Section 2. Our diagnostic of whether a nova has formed dust is presented in Section 3. In Section 4, we estimate what fraction of novae form dust and test for correlations between dust properties and other characteristics of the novae. We conclude in Section 5.

2 OBSERVATIONS

2.1 Sample of Nova Light Curves

The optical and IR light curves analysed in this paper are from the *Stony Brook / SMARTS Atlas of (mostly) Southern Novae*¹ (Walter et al. 2012). The Atlas consists of photometric and spectroscopic data of 93 novae in the Galaxy and the Magellanic clouds that erupted during \sim 2003–2019. These have measurements of varying cadence using the Johnson-Kron-Cousins B, V, R_C , and I_C filters and the CIT/CTIO J, H , and K filters. Most of the photometry was obtained using the ANDICAM dual-channel imager on the 1.3 m telescope, supplemented by some higher cadence data obtained with the SMARTS 0.9 m and 1.0 m telescopes (Walter et al. 2012). Data were reduced in a consistent manner using custom pipelines; details of the photometric observations and data reduction can be found in Walter et al. (2012). Since the uncertainties in the SMARTS photometry balloon to large values for magnitudes $\gtrsim 20$ mag, we take this as our faint detection limit, and adopt a bright saturation limit of 5 mag. We have also ignored any measurements with error ≥ 0.5 mag.

Of the 93 novae with photometry from the SMARTS Atlas, 79 have at least 20 measurements in each of the V -band and the K -band (the bands we focus on here for dust diagnostics; see Section 3.1), which we consider the minimum number of measurements for a nova to be included in our analysis. We then eliminated novae that were severely lacking in data cadence (some novae have large time gaps in their light curves) and novae that were not useful to analyse due

¹ <https://www.astro.sunysb.edu/fwalter/SMARTS/NovaAtlas/atlas.html>

to consistently high measurement errors. The literature indicates that dust events usually (≥ 90 per cent) start within the first 150 days of eruption and can last for as little as 40 days (Strope et al. 2010). All novae eliminated had a time gap of at least 50 days before day 150, during which a dust event could in theory have occurred and been missed. There are two exceptions: Nova SMC 2016 and V1311 Sco, which we both eliminate. The IR photometry of N SMC 2016 has large uncertainties, and there is a large gap in time coverage from day ~ 120 –220 during which a dust event could have occurred. V1311 Sco lacks SMARTS measurements within 27 days of eruption, during which time this rapidly evolving nova drops by ~ 7.5 mag in the V band (according to AAVSO data), which is most of the “action” of the nova eruption. We deem too much of this nova eruption was missed by the SMARTS photometry to be included in our sample.

In some cases, the K -band light curve is saturated for most of the nova eruption, including during the dust dip. For such novae, we try to complement the SMARTS data with available data in the literature. We use IR data for nova V339 Del from Burlak et al. (2015) and for nova V5668 Sgr from Banerjee et al. (2016) and Gehrz et al. (2018). SMARTS/Andicam data were re-reduced for nova V906 Car by Wee et al. (2020) and confirmed as unsaturated — we use their photometry here.

After excluding novae with poor data cadence and/or quality, we analysed 40 novae that had sufficient early observations and temporal coverage to assess dust formation. We are only considering the first year of eruption, but we expect the majority of dust forming novae to form dust over this time frame (e.g. Strope et al. 2010). According to compilations by Strope et al. (2010) and Williams et al. (2013), V445 Pup is the nova with the latest dust dip, and it began showing evidence of dust formation around day 218, with a light curve minimum around day 600 (Woudt et al. 2009); it is also a unique He nova with no H emission detected, which may contribute to its unique dust properties (Ashok & Banerjee 2003; Banerjee et al. 2023a). If an unexpected change in nova color was observed at late times, well beyond a year, the association with a dust formation event in the nova ejecta would likely be ambiguous. Therefore, we restrict our study to dust formation events in the first year of the eruption.

We present our sample of novae in Table 1, with the time of optical maximum t_{peak} and the time to decline by two magnitudes from light curve peak, t_2 . ‘Class’ lists our classification of the nova’s dust formation properties (see Section 2.2), and we also list whether the nova was detected in GeV γ -rays by the Large Area Telescope (LAT; Atwood et al. 2009) on the *Fermi Gamma-ray Space Telescope* (of course this is only feasible for novae that erupted after the launch of *Fermi*). ‘ $t_{\text{dust,start}}$ ’ refers to the earliest time in the light curve, in days (relative to t_{peak}), that we distinguish a feature in the light curve that is caused by dust formation. ‘ Δt_{dust} ’ is the time from $t_{\text{dust,start}}$ to the ‘bottom’ of the dust event, which is immediately after the ($V - K$) colour appears to have finished the large redward shift caused by dust formation. ‘ ΔV_{dust} ’ is the change in the V -band magnitude from $t_{\text{dust,start}}$ to the bottom of the dust event. The first reference(s) given under the ‘Ref.’ column (to the left of the slashes) is the source(s) where t_{peak} and t_2 are measured. In cases where the optical peak of the eruption light curve was not well-captured (i.e. there is a gap >1 week between pre-eruption non-detection

and eruption discovery), we only place an upper limit on t_2 (as most optical light curves of nova eruptions become more shallow as they evolve, barring dips caused by dust events). The second reference (between slashes in the ‘Ref.’ column) refers to the work/method used in classifying the dust formation properties. The third reference (to the right of the slashes in the ‘Ref.’ column) is the citation to the γ -ray detection or upper limit.

2.2 Categorizing Novae by Dust Properties

Each of the 40 novae in the sample were manually labelled as one of: ‘Dust Dip’, ‘IR Excess’, ‘None’, and ‘Unsure’, based on inspection of their V - and K -band light curves. In the near-IR, we focus on the K -band (rather than J/H) because it provides a longer wavelength baseline and a higher potential contrast with the V -band. This behaviour is illustrated in Figure 1, where we plot V -, J -, H -, and K -band light curves for the nova V357 Mus. This nova shows a dramatic dust dip in the V -band, bottoming out around day 65, while the K -band plateaus and even brightens a bit during this time. The J - and H -bands show ‘in between’ behaviour, where the light curves do not decline as much as the V -band during the dust dip, but do show some fading that bottoms out around day 75, likely driven by dust formation.

The ‘Dust Dip’ label refers to novae that have a brightening/plateau in the K -band, correlating with a relatively sharp decrease in V -band brightness followed by either a recovery or a plateau. V357 Mus is an example of a ‘Dust Dip’ nova (Figure 1). We note that not all of the novae in the ‘Dust Dip’ category display features that are easily distinguished as dust when looking at the V -band light curve alone. For some, it is only distinguishable when also analysing the increase in K -band brightness.

‘IR Excess’ refers to novae that have a significant brightening in the IR flux at a time when it would be reasonable for a dust event to occur, but this increase in the IR is not reflected by a significant dimming in the optical light, typically expected from dust absorption (see Figure 2 for an example). The main difference between the ‘Dust dip’ novae and ‘IR Excess’ is likely due to the location of dust formation relative to our line of sight: ‘Dust Dip’ events are referred to as *optically thick dust shells* by Gehrz (1988), marking dust that is formed in the ejecta along the line of sight, whereas ‘IR Excess’ events have been deemed *optically thin dust shells*, where newly formed dust is present but does not cover the bulk of the optical pseudo-photosphere of the nova.

The ‘None’ label refers to novae that do not display evidence of a dust formation event in their V - and K -band light curves, and for which there is enough data to assert that there was not a dust event with a reasonable degree of confidence. Figure 3 shows an example; in typical cases categorized as ‘None’, the V - and K -band light curves track one another smoothly; Moreover, the change of ($V - K$) colours as a function of time does not show an episode of reddening, and is instead observed to evolve towards the blue.

The ‘Unsure’ label is assigned to a nova that may have features of the ‘IR Excess’ or ‘Dust Dip’ categories, but these features are not pronounced enough to categorize the nova with any certainty. Novae were sometimes categorized as ‘Unsure’ if there was a gap in photometric coverage, often due to solar conjunction (e.g. N LMC 2009a; Figure 4), during

Table 1. Dust classifications for the novae included in our sample, along with the time of optical peak, t_2 , if they are detected by *Fermi*-LAT as a γ -ray source, and the properties of their dust formation feature (should it exist).

Name	t_{peak} (MJD)	t_2 (days)	Class	γ -ray detected?	$t_{\text{dust,start}}$ (days)	Δt_{dust} (days)	ΔV_{dust} (mag)	Ref.
V475 Sct	52883.8 $^{+0.5}_{-0.5}$	22 $^{+1}_{-1}$	Dust Dip	–	40.0 $^{+0.2}_{-0.7}$	76.0 $^{+1.2}_{-2.9}$	6.0	1,25/2/–
V574 Pup	53331.7 $^{+0.1}_{-0.6}$	6.6 $^{+0.2}_{-1.0}$	None	–	–	–	–	3/2/–
N LMC 2005	53710.1 $^{+1.0}_{-1.0}$	70.4 $^{+2.2}_{-2.2}$	Dust Dip	–	73.0 $^{+1.0}_{-0.1}$	110.0 $^{+2.1}_{-0.1}$	1.7	4/2/–
RS Oph (2006)	53778.9 $^{+0.1}_{-0.1}$	7.9 $^{+0.1}_{-0.1}$	None	Y ^a	–	–	–	5/6/7
N LMC 2009a	54864.5 $^{+2.5}_{-2.5}$	7.0 $^{+2.7}_{-2.7}$	Unsure	–	–	–	–	8/2/–
N LMC 2009b	–	–	Dust Dip	–	50.0 $^{+17.5b}_{-39.0}$	90.0 $^{+25.4b}_{-39.0}$	3.9 ^b	–/2/–
V5584 Sgr	55138.4 $^{+1.4}_{-2.0}$	40.7 $^{+142.1}_{-27.3}$	Dust/Unsure ^c	N	–	–	–	9/2/10
V5588 Sgr	55658.1 $^{+1.0}_{-1.0}$	46.0 $^{+1.4}_{-1.0}$	None	N	–	–	–	9/2/10
V1312 Sco	55714.3 $^{+0.2}_{-3.3}$	12.9 $^{+1.3}_{-3.4}$	None	N	–	–	–	9/2/10
PR Lup	55787.4 $^{+0.7}_{-0.2}$	14.7 $^{+0.7}_{-0.6}$	Dust/Unsure ^c	N	–	–	–	9/2/10
V834 Car	55987.4 $^{+0.1}_{-0.2}$	20.1 $^{+0.1}_{-0.2}$	None	N	–	–	–	8/2/10
N LMC 2012a	56006.4 $^{+6.0}_{-6.0}$	<2.0	None	–	–	–	–	11/2,11/–
V1368 Cen	56008.5 $^{+1.8}_{-1.8}$	16.1 $^{+1.8}_{-1.8}$	Dust Dip	N	36.0 $^{+4.7}_{-2.3}$	70.0 $^{+6.6}_{-3.4}$	2.1	12/2/10
V2676 Oph	56021.5 $^{+1.9}_{-1.0}$	83.8 $^{+2.1}_{-1.4}$	Dust Dip	N	85.0 $^{+2.8}_{-1.2}$	100.0 $^{+5.5}_{-1.2}$	7.4	9/2/10
V1428 Cen	56024.8 $^{+0.5}_{-0.4}$	10.8 $^{+0.9}_{-0.5}$	IR Excess	N	20.0 $^{+4.4}_{-4.7}$	55.0 $^{+5.6}_{-6.0}$	5.0	9/2/10
V5589 Sgr	56039.5 $^{+0.1}_{-1.6}$	2.3 $^{+0.6}_{-1.6}$	None	N	–	–	–	9/2/10
V2677 Oph	56068.3 $^{+0.2}_{-2.6}$	6.7 $^{+0.3}_{-2.7}$	None	N	–	–	–	9/2/10
V1324 Sco	56098.0 $^{+0.4}_{-0.3}$	24.2 $^{+0.4}_{-0.3}$	Dust Dip	Y	19.0 $^{+0.2}_{-2.7}$	47.0 $^{+0.2}_{-5.5}$	8.9	9/2/13
V5591 Sgr	56105.3 $^{+0.2}_{-0.7}$	2.3 $^{+0.3}_{-0.7}$	None	N	–	–	–	9/2/10
V5592 Sgr	56115.5 $^{+4.3}_{-4.3}$	<16.8	Dust Dip	N	15.0 $^{+15.2}_{-1.7}$	44.0 $^{+15.2}_{-13.9}$	6.4	12,14/2/10
V1533 Sco	56447.5 $^{+0.7}_{-3.8}$	7.9 $^{+3.1}_{-3.9}$	IR Excess	N	14.0 $^{+1.9}_{-1.2}$	26.0 $^{+2.6}_{-1.7}$	1.5	9/2/10
V339 Del	56520.7 $^{+0.1}_{-0.5}$	11.3 $^{+0.4}_{-0.5}$	Dust Dip	Y	27.0 $^{+2.4}_{-7.6}$	55.0 $^{+2.7}_{-7.6}$	2.5	9,26/2/13
N LMC 2013	56577.3 $^{+4.0}_{-4.0}$	52 $^{+4.9}_{-4.1}$	Dust Dip	–	48.0 $^{+2.9}_{-0.1}$	110.0 $^{+4.0}_{-4.2}$	2.6	15,16/2/–
V1369 Cen	56640.7 $^{+2.0}_{-1.9}$	37.7 $^{+2.4}_{-4.1}$	IR Excess	Y	30.0 $^{+6.7}_{-11.3}$	78.0 $^{+6.7}_{-11.3}$	2.7	9/2/17
V745 Sco (2014)	56694.8 $^{+1.1}_{-0.1}$	2.5 $^{+1.1}_{-0.5}$	IR Excess	N ^d	5.5 $^{+0.1e}_{-0.9}$	13.0 $^{+0.6e}_{-1.0}$	3.3 ^e	18/23/10
V5666 Sgr	56705.4 $^{+1.0}_{-1.0}$	68.5 $^{+1.1}_{-1.1}$	Unsure	N	–	–	–	12/2/10
V1534 Sco	56744.5 $^{+1.1}_{-1.1}$	5.6 $^{+1.4}_{-1.4}$	None	N	–	–	–	19/2,24/10
V1535 Sco	57064.3 $^{+1.1}_{-1.1}$	9.2 $^{+1.4}_{-1.4}$	None	N ^d	–	–	–	19/2/10
V5667 Sgr	57068.7 $^{+2.0}_{-0.9}$	64.0 $^{+2.0}_{-1.3}$	Unsure	N	–	–	–	9/2/10
V5668 Sgr	57102.4 $^{+0.3}_{-0.3}$	74.7 $^{+3.3}_{-3.8}$	Dust Dip	Y	75.0 $^{+6.0}_{-4.1}$	105.0 $^{+6.7}_{-4.2}$	6.7	9/2/17
V2944 Oph	57125.6 $^{+1.0}_{-1.0}$	32.5 $^{+1.1}_{-1.2}$	Unsure	N	–	–	–	20/2/10
V3661 Oph	57459.8 $^{+1.1}_{-1.1}$	3.9 $^{+1.4}_{-1.4}$	Unsure	–	–	–	–	19/2/–
V3662 Oph	57873.2 $^{+3}_{-1}$	37.0 $^{+6.7}_{-5.7}$	Dust Dip	–	45.0 $^{+4.0}_{-0.1}$	60.0 $^{+4.5}_{-0.1}$	4.0	9/2/–
V1405 Cen	57891.5 $^{+2.0}_{-1.0}$	108.5 $^{+5.4}_{-14.1}$	None	–	–	–	–	12/2/–
V612 Sct	57964.0 $^{+0.9}_{-1.0}$	132.2 $^{+78.2}_{-12.5}$	Unsure	N	–	–	–	9/2/9
V357 Mus	58134.4 $^{+1.1}_{-11.1}$	22.9 $^{+1.6}_{-11.1}$	Dust Dip	Y	20.0 $^{+1.9}_{-0.1}$	65.0 $^{+3.3}_{-3.3}$	10.3	9/2/21
V1661 Sco	58136.8 $^{+1.1}_{-1.1}$	11.2 $^{+3.2}_{-4.2}$	Dust Dip	–	13.0 $^{+2.6}_{-13.0}$	55.0 $^{+3.0}_{-13.1}$	6.2	9/2/–
FM Cir	58146.3 $^{+1.0}_{-0.9}$	133.7 $^{+1.0}_{-2.2}$	Unsure	N	–	–	–	9/2/9
V1662 Sco	58159.3 $^{+1.1}_{-1.1}$	14.5 $^{+1.1}_{-0.7}$	IR Excess	–	14.0 $^{+0.6}_{-1.5}$	47.0 $^{+1.6}_{-1.6}$	4.3	9/2/9
V906 Car	58205.5 $^{+1.0}_{-0.9}$	43.7 $^{+1.3}_{-1.1}$	IR Excess	Y	20.0 $^{+0.6}_{-0.4}$	75.0 $^{+2.6}_{-1.6}$	2.9	9/2/22

References (light curve parameters/ dust classification/ *Fermi*/LAT detection): 1=Morgan et al. (2005); 2= This work; determined using *V* and *K* band light curves; 3=Samus & Kazarovets (2004); 4= Liller et al. (2007); 5=Hounsell et al. (2010); 6=Evans et al. (2007); 7=Cheung et al. (2022); 8=Bode et al. (2016); 9= Craig et al. 2025, in preparation; 10=Franckowiak et al. (2018); 11= Schwarz et al. (2015); 12= Measured here using AAVSO and ASAS-SN light curves; 13=Ackermann et al. (2014); 14=Nishimura & Nakano (2012); 15=Wyrzykowski et al. (2013); 16= Measured from OGLE I Band light curve Mróz et al. (2016); 17=Cheung et al. (2016); 18= Molina et al. 2024, accepted; 19=Munari et al. (2017); 20=Srivastava et al. (2016); 21=Gordon et al. (2021); 22=Aydi et al. (2020a); 23=Banerjee et al. (2023b); 24=Joshi et al. (2015); 25=Chochol et al. (2006); 26=Gehrz et al. (2015)

^a While the 2006 eruption of the recurrent nova RS Oph was not observed with *Fermi*/LAT, the 2021 eruption was, and was detected.
^b Values are relative to the time of discovery for N LMC 2009b (MJD 54956.0; Liller & Monard 2009) due to a lack of data around light curve peak. ^c While we are unsure if V5584 Sgr and PR Lup are ‘Dust Dip’ or ‘IR Excess’ novae, it is clear that they formed dust.
^d Marginal, sub-threshold hints of detection are seen in *Fermi*/LAT (Franckowiak et al. 2018).

^e V745 Sco continues to redden after the dust event concludes, due to the system’s red giant companion star; for this nova, Δt_{dust} is the time from $t_{\text{dust,start}}$ to when the small bump in the *K*-band caused by the dust event has ended (Banerjee et al. 2023b).

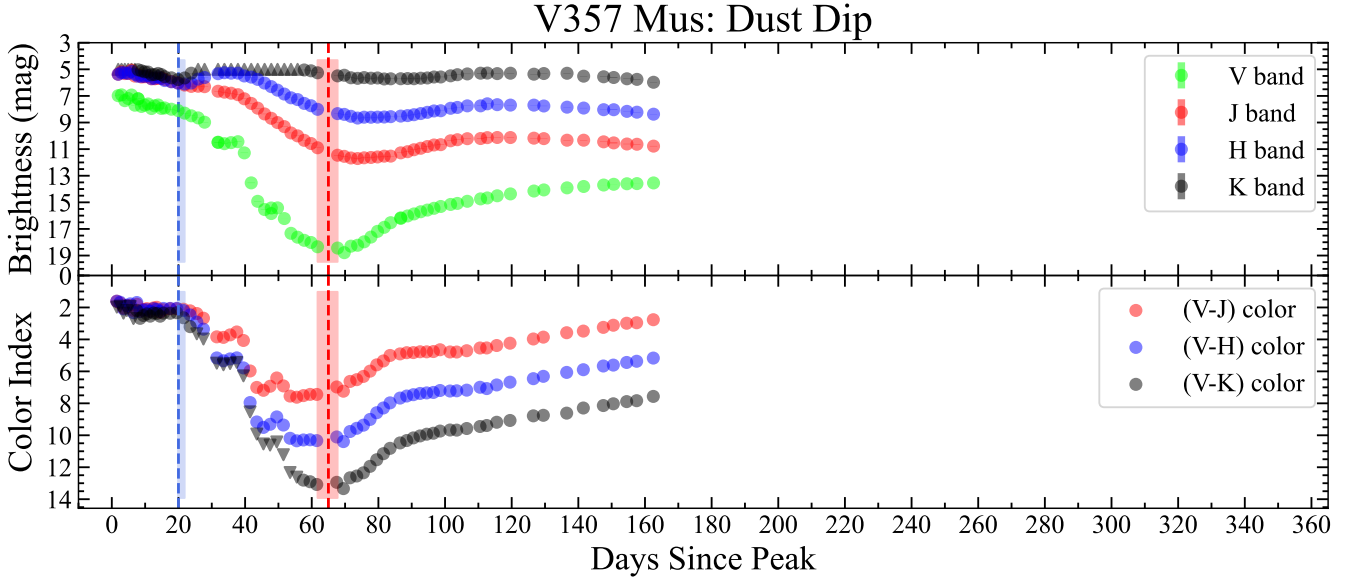


Figure 1. Example V , J , H , and K light curves, and corresponding colour curves of nova V357 Mus, which we classify as ‘Dust Dip’. Its V -band light curve dramatically declines and bottoms out around day 65, while the K -band light curve remains relatively constant and even increases a bit during the V -band dust dip. J - and H -bands show behaviour intermediate to that of V - and K -bands. The blue vertical bar denotes the earliest feature attributable to the dust event (in this case, a rise in the K -band light curve), while the red vertical bar marks the largest redward excursion of the $(V - K)$ colour (i.e., the ‘bottom’ of the dust dip). The width of the bars is set by the cadence of the photometry at these times.

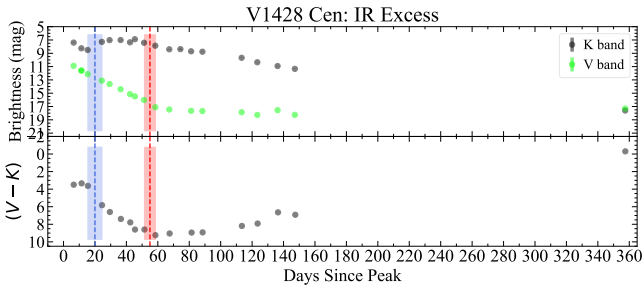


Figure 2. Example V and K light curves, and $(V - K)$ colour curve, of a nova that has been classified as ‘IR Excess’: V1428 Cen. Its V -band light curves shows a smooth decline while the K -band light curve increases in flux around day 20. The $(V - K)$ colour curve shows a clear reddening over the course of this dust formation episode. As in Figure 1, the blue bar marks the start of the dust dip and the red bar marks the reddest point in the $(V - K)$ curve.

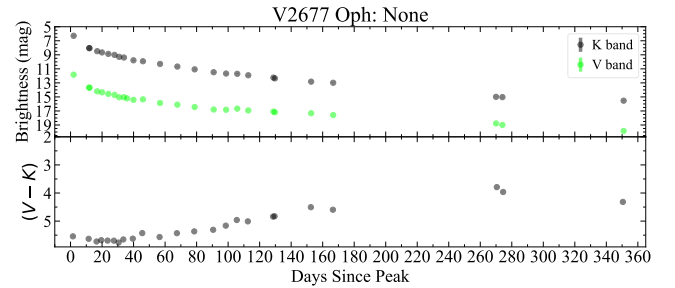


Figure 3. Example V and K light curves, and $(V - K)$ colour curve, of a nova that has been classified as ‘None’: V2677 Oph. Both the V and K light curves monotonically decline from maximum and $(V - K)$ smoothly evolves towards bluer colours.

which a dust formation event could have occurred, or if there were relatively mild features in the $(V - K)$ colour evolution which were not accompanied by clear dips/excesses in the light curves (e.g. V5667 Sgr; Figure 5). In categorizing the novae, we erred to an ‘Unsure’ label when we were uncertain about classification, in order to avoid introduction of bias.

In the cases of most ‘Unsure’ novae, we are unsure if they formed dust. V5584 Sgr and PR Lup are exceptions in that they almost certainly formed dust, but due to large observation gaps caused by solar conjunction, we did not capture the dust formation episodes. We therefore classify them as ‘Dust/Unsure’, but they are almost certainly either ‘Dust Dip’ or ‘IR Excess’, based on the large change in the $(V - K)$ colour during the solar conjunction. The light curves and

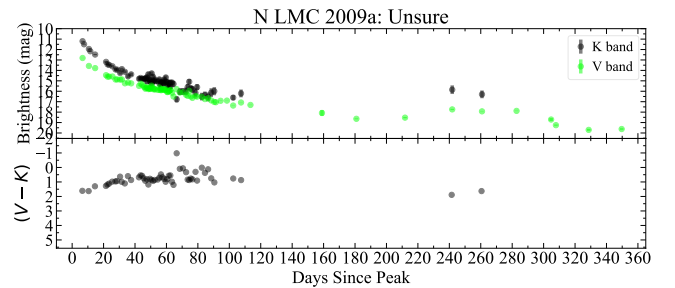


Figure 4. Example V and K light curves, and $(V - K)$ colour curve, of a nova that has been classified as ‘Unsure’: N LMC 2009a. It has a gap in photometric coverage during which a dust formation event could have occurred.

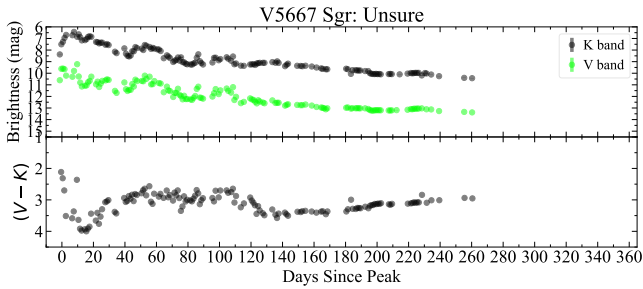


Figure 5. Example V and K light curves, and $V - K$ colour curve, of another nova that has been classified as ‘Unsure’: V5667 Sgr. It shows some change in $V - K$ colour but has no clear features associated with the colour change in the V and K light curves that would distinguish a dust event.

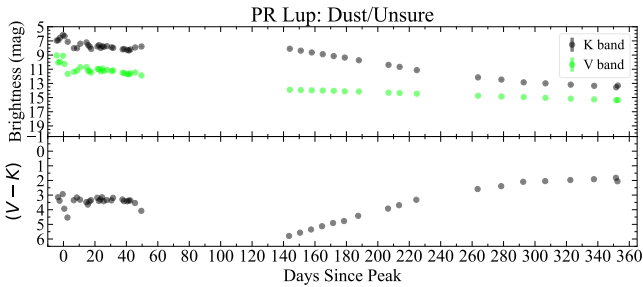


Figure 6. V and K light curves, and $(V - K)$ colour curve, for PR Lup. PR Lup almost certainly formed dust, but it is unclear if it should be classified as ‘IR Excess’ or ‘Dust Dip’ due to a large gap in observations around solar conjunction.

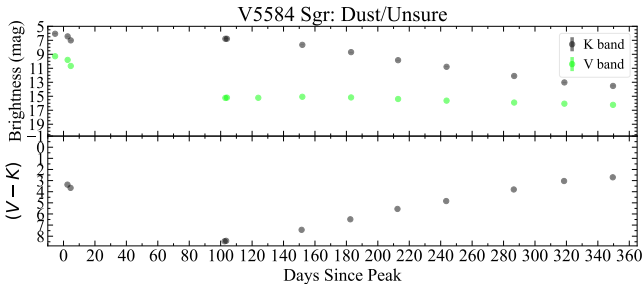


Figure 7. V and K light curves, and $(V - K)$ colour curve, for V5584 Sgr. V5584 Sgr almost certainly formed dust, but it is unclear if it should be classified as ‘IR Excess’ or ‘Dust Dip’ due to a large gap in observations around solar conjunction.

colour plots of PR Lup and V5584 Sgr can be found in Figure 6 and Figure 7 respectively.

In cases where there is additional evidence from the literature (i.e., spectroscopy) that supports a nova forming dust or not, we take this information into account in our dust classification. Take for example, the recurrent nova RS Oph; while dust has been detected in the binary, IR spectroscopy and imaging suggests that the silicate grains have been processed and therefore likely originate in the red giant companion’s wind (Evans et al. 2007; Barry et al. 2008); we therefore classify it as ‘None’. On the other hand, another recurrent nova with a red giant companion, V745 Sco, was suggested to have formed dust based on detection of broad CO lines

in IR spectra, which are concurrent with a relatively subtle increase in the IR brightness between day 8 and 10 after visible peak (Banerjee et al. 2023b). While we do not believe V745 Sco shows strong evidence of dust formation from the SMARTS data alone, Banerjee et al. point out that ‘all novae that have shown CO in emission have invariably proceeded to form dust’, so we classify it as ‘IR Excess’ here. Yet another nova with a likely giant companion, V1534 Sco, was monitored with IR spectroscopy and showed no CO emission or other signs of dust formation (Joshi et al. 2015); it is classified here as ‘None’.

In summary, our sample contains 13 ‘Dust Dip’ novae (32.5 per cent), 6 ‘IR Excess’ novae (15 per cent), 2 ‘Dust/Unsure’ novae (5 per cent), 12 ‘None’ novae (30 per cent), and 7 ‘Unsure’ novae (17.5 per cent). Therefore, out of the 40 novae in our sample, 21 show signatures of dust formation in their light curves (including PR Lup and V5668 Sgr). Plots like Figures 1–7, showing the V and K light curves and colour curves, are available for all 40 novae in Appendix A (Figures A.1–A.40).

3 DIAGNOSTICS OF DUST FORMATION

3.1 $(V - K)$ Colour Diagnostic

Colour curves, comparing an optical band with a near-IR band as a function of time, are particularly useful for distinguishing dust formation events in novae. Dust should cause the optical band to dim and the near-IR band to plateau or brighten, so their difference should be even more affected by dust than the optical or near-IR light curves alone. From visual inspection of the near-IR JHK -band light curves for our novae, it is clear that the K -band is the most likely to show an excess in flux at the time of dust formation, and provides the strongest contrast with the V -band light curve (e.g. Figure 1). We therefore begin our search for a simple diagnostic of dust formation in novae by analysing the $(V - K)$ colour curves. How the $(V - K)$ colour changes with time has potential to be a powerful indicator of dust formation, especially because it is insensitive to interstellar reddening.

Using the $(V - K)$ colour curves, we have separated the dust-forming novae and novae with no evidence of dust formation into distinct, non-overlapping groups, as shown in Figure 8. To calculate the vertical axis of Figure 8, we take the $(V - K)$ colour around V -band light curve peak, as measured in the SMARTS data (see Figures A.1–A.40). Because of the limited cadence of the SMARTS data, sometimes these are offset in time from the true light curve peak by several days, with several novae having greater offsets; V574 Pup has the largest offset of 30 days. The average offset is 5.9 days, and the median is 3.1 days. We explore in Appendix B how quickly and dramatically the $(V - K)$ colour changes around peak, and conclude that the SMARTS photometry is of sufficient cadence to constrain the colour near peak. We then measure the greatest redward excursion from this peak colour, as observed over the first year of eruption. It is this largest redward change in $(V - K)$ colour that is plotted on the y-axis of Figure 8. Novae where the K -band light curve saturates or the V -band light curve drops below detectability are plotted as lower limits on the $(V - K)$ change. On the horizontal axis of Figure 8 we plot the time it took for this

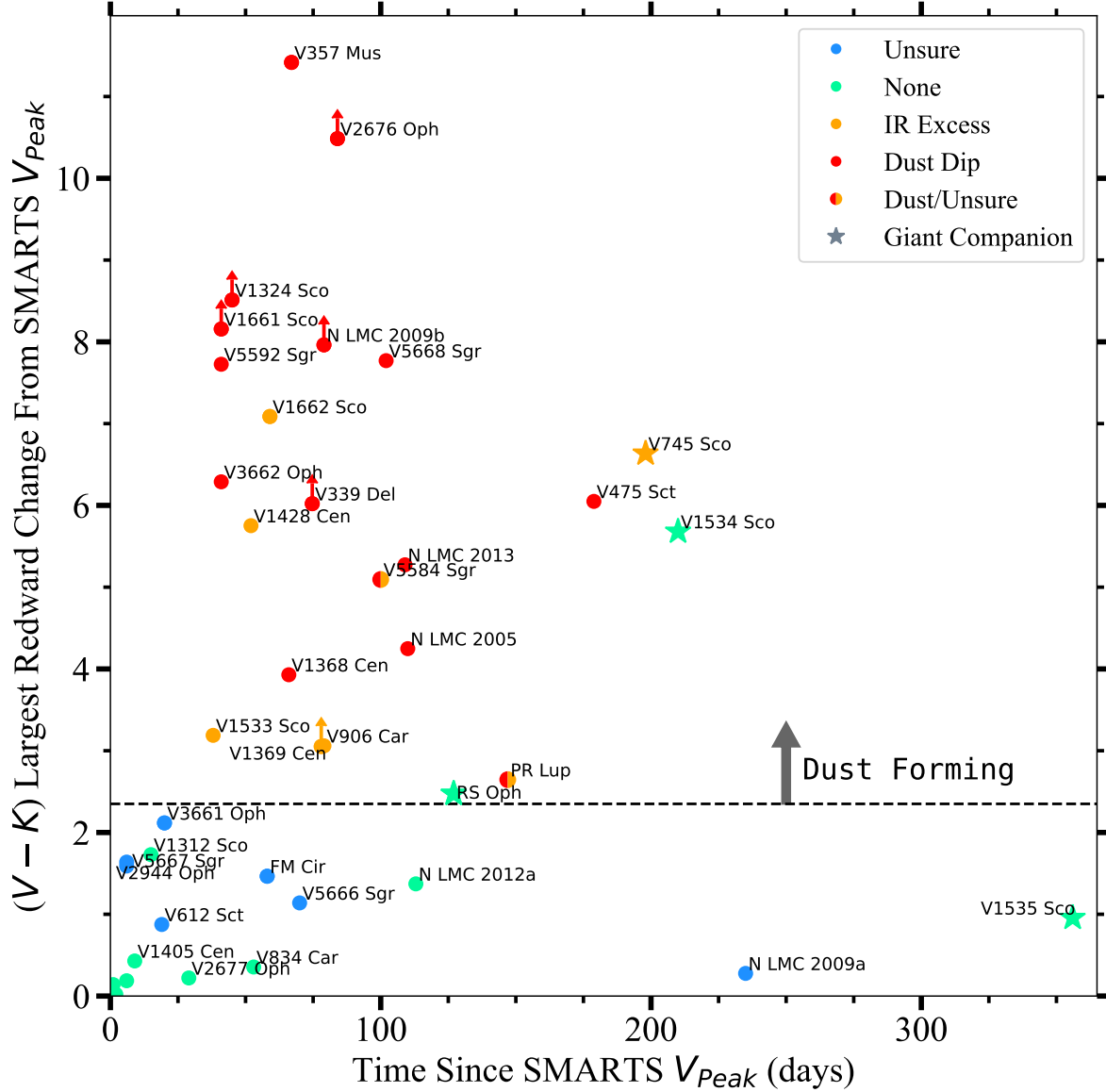


Figure 8. A plot summarizing our recommended $(V - K)$ dust formation diagnostic. On the y-axis is plotted the largest redward change in the nova’s $(V - K)$ colour compared to its colour at SMARTS V -band light curve peak. On the x-axis is plotted the time for this colour change to occur. Novae with dust features in their light curves (red and orange dots) are clustered in the upper left corner of the plot, while novae without dust features (cyan dots) are mostly in the lower portion of the plot. The horizontal line at a $(V - K)$ colour change of 2.35 mag does a good job separating novae that form dust from novae that do not. Novae with giant companions complicate this separation, and are denoted as stars rather than dots. Novae in the bottom left corner of the plot are too crowded for labels, and include V574 Pup, V5591 Sgr, V5589 Sgr, and V5588 Sgr.

change in colour to occur. V1428 Cen (Figure 2), for example, is at 5.75 mag on the vertical axis and 52 days on the horizontal axis, as the most extreme change in $(V - K)$ colour is 5.75 mag between day ~ 6 (the time of SMARTS V -band maximum) and day 58.

Novae that form dust, be they ‘Dust Dip’ novae (red dots) or ‘IR Excess’ novae (orange dots), dwell in the upper portion of Figure 8, implying a large redward colour diversion. This region of the plot is characterized by a change in $(V - K)$ from peak of > 2.35 mag (marked as a horizontal dashed line). Most of the ‘None’ novae (cyan dots) are significantly removed from this upper cluster of dust-forming novae and are found near the bottom of the plot. **Our best single di-**

agnostic for dust formation in novae is an observation of $(V - K)$ colour that is > 2.35 mag redder than at peak.

V1534 Sco and RS Oph, the two cyan ‘None’ points found in the top (dust-forming) portion of the plot, are both systems that have a red giant companion star and as such redden significantly when approaching quiescence (Brandt et al. 2009; Joshi et al. 2015; Munari & Banerjee 2018). We also note evidence suggesting that V1535 Sco, found on the bottom-far right of Figure 8, also has a red giant companion star (Linford et al. 2017).

We note that sometimes novae are missed during light curve peak, due to solar conjunction or other gaps in cov-

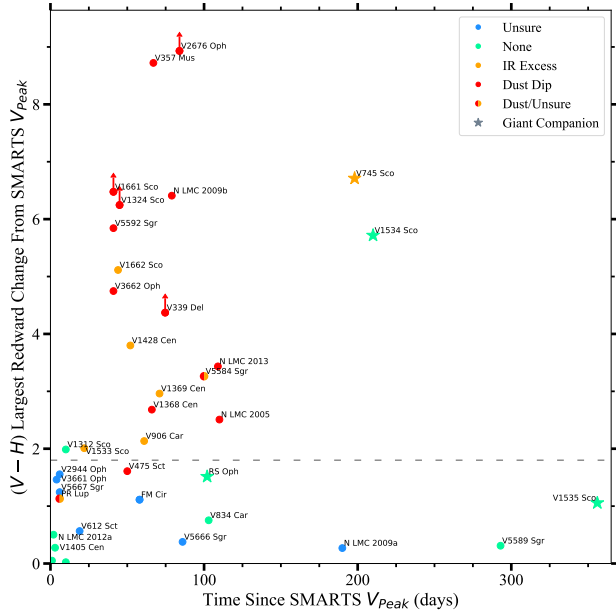


Figure 9. A plot similar to Figure 8, except with the H -band in place of the K -band. We include a dotted line at a $(V - K)$ colour change of 1.8 that mostly separates the dust-forming from the non-dust-forming novae. Note that the light curves for both PR Lup and V475 Sct do not capture the ‘bottom’ of the dust event in both V -band and K -band, and as such both novae appear lower on the plot than they would with better coverage. V5668 Sgr is not included due to H -band saturation near peak and during its dust dip. Novae in the bottom left corner of the plot are too crowded for labels, and include V2677 Oph, V5588 Sgr, V5591 Sgr, and V574 Pup.

erage. A recent extreme example is the 2020 nova YZ Ret, which peaked at visual magnitude 3.7 but was noticed only a week after the eruption (Sokolovsky et al. 2022). Our recommended dust diagnostic can still be used in these cases if later V and K light curves are obtained, the interstellar reddening to the nova is measured, and the typical intrinsic $(V - K)_0$ colour of a nova at peak is known. For this reason, we estimate $(V - K)_{0,\text{peak}}$ in Appendix C, and find it, on average, to be 1.1 with a standard deviation of 0.8 mag. The implication is that, if a nova eruption exhibits an intrinsic $(V - K)_0 > 5.1$ during its evolution, it is likely (at the 2σ level) to have formed dust.

3.2 Can dust formation be diagnosed from J - and H -bands?

We do not expect the excess in IR flux that accompanies dust formation to be as dramatic in the J - and H -bands compared to K -band (Figure 1; e.g., Szkody et al. 1979; Bode et al. 1984; Arai et al. 2010; Aydi et al. 2019). And yet, wide-field time-domain surveys like WINTER and PRIME are being carried out in the J - and H -bands respectively, and should produce high-quality near-IR light curves for a large fraction of Galactic novae. Can we use these J - and H -band data sets to diagnose dust formation in novae?

Figures 9 and 10 are plots of the largest redward colour change from V -band peak vs Δt (similar to our $(V - K)$ di-

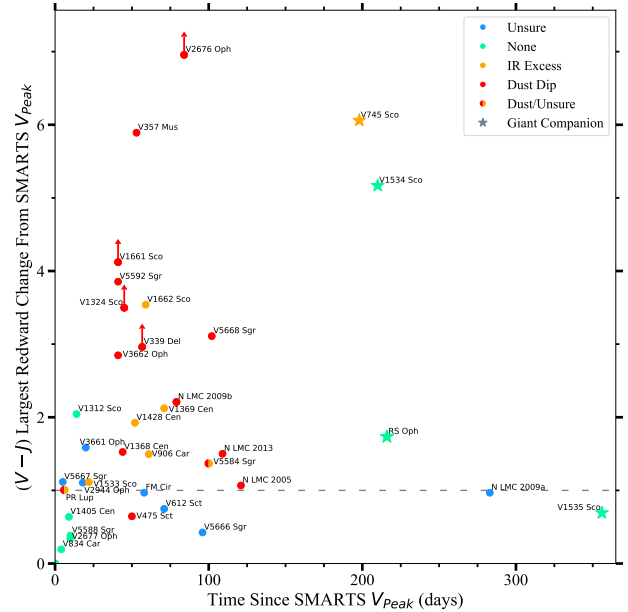


Figure 10. Same as Figure 8 but for $(V - J)$ colours. There is no longer a clear separation between the ‘None’-dusty novae and novae with dust features. We include a dotted line at a $(V - K)$ colour change of 1.0 that mostly separates the dust-forming from the non-dust-forming novae. Note that the light curves for both PR Lup and V475 Sct do not capture the ‘bottom’ of the dust event in both V -band and K -band, and as such both novae appear lower on the plot than they would with better coverage. Novae in the bottom left corner of the plot are too crowded for labels, and include N LMC 2012a, V5589 Sgr, V5591 Sgr, and V574 Pup.

agnostic plot; Figure 8) for $(V - H)$ and $(V - J)$, respectively. As in Figure 8, the dust-forming novae tend to sit towards the tops of these plots, and the ‘None’ novae dwell towards the bottoms. However, the vertical separation between dust-formers and non-dust-formers is not as clear in these plots. A $(V - H)$ reddening from peak of >1.8 captures nearly all dust-forming novae, but also includes the ‘None’ nova V1312 Sco (Figure A.9). A $(V - J)$ reddening of >1.0 similarly includes nearly all dust-forming novae, but also includes V1312 Sco and three ‘Unsure’ novae. Note that the light curves for both PR Lup and V475 Sct do not capture the ‘bottom’ of the dust event in J -band and K -band, and as such both novae appear lower on the plot than they would with better coverage. Therefore, while the J - and H -bands can be used in concert with optical photometry to assess whether a nova is likely to have formed dust, the false positive rate is likely to be higher than if one instead uses $(V - K)$ as a diagnostic.

Condensation temperature estimates for dust commonly seen in nova ejecta range from 1150 K to 1720 K, with a median of 1325 K (Ebel 2000; Evans & Rawlings 2008), which we can use as a rough estimate for the temperature at which grains will form. It is not unreasonable to expect multiple species of dust in the wind of a single nova which can generate a complex IR spectral energy distribution (SED), but the condensation temperature can give us an upper bound on the peak of the dust thermal re-emission SED. The blackbody curve for 1325 K peaks at $2.19 \mu\text{m}$, which is within the K -band ($1.99 - 2.30 \mu\text{m}$) but redward of the J - and H -bands

(1.16 – 1.33 μm and 1.47 – 1.79 μm , respectively). Thermal radiation at that temperature would still cause an increase in the J - and H -bands, but not as large or easily measured as the change in the K -band. At cooler temperatures, dust re-emission may not be detectable in the J -band, while still having a noticeable effect in the K -band.

As in Section 3.1, it may be useful to know the intrinsic $(V - J)_0$ and $(V - H)_0$ of nova eruptions at peak; this could enable the assessment of whether a nova forms dust even if no photometry is obtained around light curve peak. We estimate these colours around peak for novae in our sample with good measurements of interstellar reddening in Appendix C, finding $\langle (V - J)_{0,\text{peak}} \rangle = 0.8 \pm 0.6$ and $\langle (V - H)_{0,\text{peak}} \rangle = 0.7 \pm 0.6$. Combined with the color-change diagnostics of Figures 9 and 10, we conclude that if a nova reaches an intrinsic $(V - J)_0 > 3.0$ or $(V - H)_0 > 3.7$ during its eruption, it likely ($>95\%$) formed dust.

4 DISCUSSION

4.1 Do slower novae form dust more often than faster novae?

We assess how the likelihood that a nova forms dust depends on its speed class, t_2 , in Figure 11. It is a histogram that divides the novae in our sample into four speed class bins—*very fast*: $t_2 \leq 10$ days; *fast*: $t_2 = 11$ –25 days; *moderately fast*: $t_2 = 26$ –80 days; and *slow*: $t_2 = 81$ –150 days (Payne-Gaposchkin 1957). Our results show that for the very fast nova group, 67 $^{+10}_{-15}\%$ per cent do not show dust, with only 17 $^{+16}_{-6}\%$ per cent of them showing clear signatures of dust formation (error bars assume binomial uncertainty with Bayesian confidence intervals calculated as in Cameron 2011). In contrast, for the fast and moderately fast novae, the majority (75 $^{+8}_{-16}\%$ per cent and 70 $^{+10}_{-17}\%$ per cent, respectively) show signatures of dust formation. Slow novae, with t_2 between 81 and 150 days, tend to be rare, and there are not enough data to draw clear conclusions about this class.

Figure 12 shows the t_2 distributions of the different dust classes of novae in more detail. We see that there is a very strong transition from novae that do not form dust to those that do around the $t_2 = 10$ days mark. Our data are consistent with 85 per cent of novae with $t_2 \leq 10$ days not hosting a dust formation episode (Table 1). While the general trend of the fastest novae being less likely to produce dust has been commented on for decades (e.g. Gallagher 1977; Williams et al. 2013), the data presented here are the clearest indication of this trend, incorporating high-quality IR data for a significant sample of novae, that we are aware of.

What might explain this trend of slower evolving novae being more likely to form dust than very fast novae? To first order, the trend seems reasonable given that the ejecta in very fast novae tend to have lower mass and more rapid expansion velocities, implying lower densities (Shara 1981; Yaron et al. 2005; Aydi et al. 2020b). This means that it is more difficult for dust to condense in the ejecta of such novae (e.g. Rawlings 1988). The lower density of the ejecta also means that it is difficult to shield the dust from the irradiation by the central source, which could lead to rapid dust destruction. In contrast, slower evolving novae where the ejecta are expected to be more massive and more slowly expanding, could allow

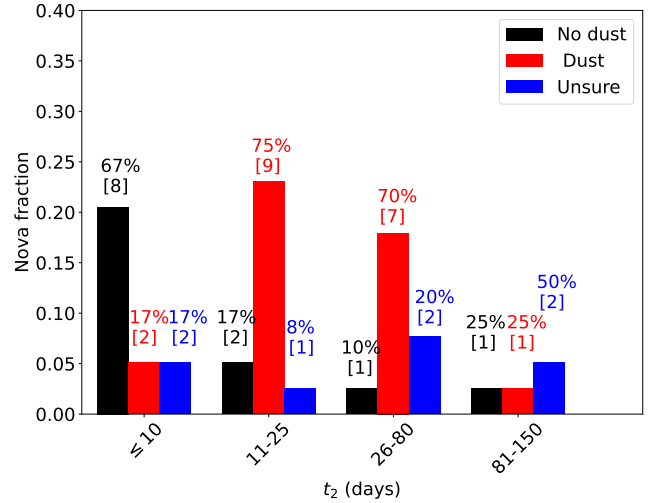


Figure 11. Bar chart comparing the fraction of novae that form dust as a function of speed class. Black bars represent novae that do not show dust formation, red bars represent novae with evidence for dust formation, and blue bars represent novae that are unsure. The errors on the percentages are the following, from left to right: 67 $^{+10}_{-15}\%$, 17 $^{+16}_{-6}\%$, 17 $^{+16}_{-6}\%$, 17 $^{+16}_{-6}\%$, 75 $^{+8}_{-16}\%$, 8 $^{+15}_{-3}\%$, 10 $^{+17}_{-3}\%$, 70 $^{+10}_{-17}\%$, 20 $^{+17}_{-7}\%$, 25 $^{+27}_{-10}\%$, 25 $^{+27}_{-10}\%$, and 50 $^{+20}_{-20}\%$ (see Section 4.1).

dust to condense and to be shielded from the irradiation by the central white dwarf.

There is the additional factor that very fast novae will be more likely to occur on massive white dwarfs composed of O and Ne, rather than C and O. These elements are mixed from the white dwarf into the nova ejecta, as indicated by spectroscopy in the optical-IR (Gehrz et al. 1998; Helton et al. 2012) and X-ray (e.g., Sokolovsky et al. 2020). There is a possibility that dust forms more readily in ejecta polluted with C/O (i.e. carbon grains) rather than O/Ne (i.e. silicate grains). Finally, there is the possibility that very fast novae host less energetic or less frequent shocks in their ejecta than slower novae, which could imply diminished dust formation if radiative shocks are the sites of dust formation in novae (Derdzinski et al. 2017). However, the fastest nova observed to date, the 2021 eruption of V1674 Her with $t_2 = 1.1$ days, displayed prominent shock signatures in both γ -rays and radio (Sokolovsky et al. 2023), and it was not reported to form dust (Woodward et al. 2021; Habtie et al. 2024).

There is also the possibility that more very fast novae form dust than are currently recognized, because the signatures of dust formation are subtle and short-lived. The dust formation in the very fast nova V745 Sco was only recognized because of IR spectroscopy, wherein Banerjee et al. (2023b) observed broad molecular CO emission lines associated with the nova ejecta. They also associate the presence of CO with a small bump in the K-band light curve that lasts between one and two weeks, but such inferences would have been near impossible from photometry alone. Relatively high cadence IR spectroscopy of very fast novae is needed to constrain the prevalence of rapid, subtle dust-forming episodes like that seen in V745 Sco. In addition, optical spectral line profiles also have the potential to reveal dust in nova ejecta, even

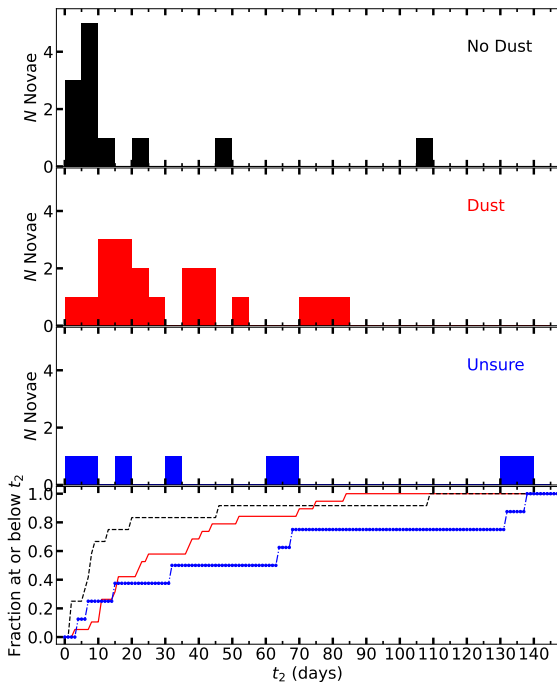


Figure 12. *Top 3 panels:* histograms showing the number of novae as a function of t_2 , divided into 5-day bins. The novae with no evidence of dust formation are presented in the *top* panel using black bars. The dust-forming novae (including both dust dip and IR excess) are presented in the *second-from-top* panel using red bars, and the ‘Unsure’ novae are presented in the *third-from-top* panel using blue bars. *Bottom panel:* cumulative distributions of t_2 values, plotted for each of the three groups (non-dust forming nova are plotted as a black dashed line, dust forming novae as a red solid line, and unsure novae as a blue dotted line).

long after the optical dust dip and/or IR excess have passed (Shore et al. 2018).

4.2 The fraction of novae that form dust

Among the 40 novae in our sample, we can confirm that a bit over half of them show evidence for dust formation, whether through a dip in the optical light curve (13 novae) or an IR excess (8 novae, including PR Lup and V5584 Sgr). For another 7 of the novae in our sample, we cannot confirm whether they formed dust or not due to them not having the typical smoothly-declining light curves we associate with non-dust-producing novae while still lacking clear features distinguishing dust formation. For the remaining 12 novae, we see no evidence for dust formation in the light curves. This means that at least 53 ± 8 per cent of the novae in our sample form dust (again, taking binomial uncertainty with Bayesian confidence intervals). Taking into account the novae classified as ‘Unsure’, the fraction of novae that form dust is at most 70_{-8}^{+6} per cent. Excluding LMC novae and focusing on Milky Way novae alone, we find the same result: at least 53 ± 8 per cent of the Galactic novae in our sample formed dust. These statistics imply that a significant number of novae—likely the majority—do form dust.

Strope et al. (2010) analysed the light curves of 93 novae and found that only 18 per cent of them show dust dips,

which is less than half of what our results show. One reason for this discrepancy could be due to the method used to classify a dust event in a light curve. Strope et al. (2010) relied on V -band light curves to classify dust dips, making it challenging to identify dust formation episodes unless they are pronounced in optical bands. Here, we instead use multi-band light curves (in both optical and near-IR) and make use of colours to help us better identify dust dips, enabling us to identify dust formation episodes that are not as pronounced or obvious. V -band light curves alone are not ideal for deriving an estimate of the total percentage of dust-forming novae in a sample, since our results show that around 15 per cent of novae show IR excess only, without a significant dust dip in the optical. However, even if we limit our sample to the ‘Dust Dip’ novae which show clear V -band dips more similar to the selection criteria in Strope et al. (2010), this is still about 35 ± 8 per cent, higher than their value of 18 per cent at about 2σ .

50–70 per cent of novae in our sample form dust, and now we consider whether this fraction holds for classical novae generally. In principle, a selection bias in the Stony Brook/SMARTS-observed sample of novae could affect our estimate of the overall fraction of novae that form dust. In the previous subsection (Section 4.1) we show that the fastest novae are less likely to form dust, suggesting that a bias in our sample’s distribution of nova speed-classes could affect our derived dust fraction. The Stony Brook/SMARTS Atlas, from which we draw our sample, deliberately targets He/N, recurrent, and LMC novae (Walter et al. 2012). Since these types typically exhibit faster optical light curves, our sample may over-represent the fastest novae. To test if we are biased in speed class, we compare the distribution of speed classes in our sample with that of Craig et al. 2025 (in preparation), who take a sample of novae that erupted during 2008–2021 and consistently measure t_2 values (primarily from AAVSO data; Kloppenborg 2023); the Craig et al. sample is a reasonable representation of the population of novae discovered during the last two decades. Our sample consists of 33/31/26/10 per cent in the very fast, fast, moderately fast, and slow speed classes respectively, whereas the 50 novae in the Craig et al. sample are distributed as 28/32/26/14 per cent amongst these speed classes. These two distributions are essentially identical, within sampling errors, implying that the sample of novae considered here represents the currently discovered Galactic population well. Hence, speed class distribution is unlikely to be significantly biasing our estimate of the fraction of novae that form dust.

Not only could the sample we use for this study be biased in terms of t_2 , but the overall population of Galactic novae our broad community discovers could also be biased in terms of t_2 . In recent years there have been several works arguing that faint, fast novae comprise a significant fraction of all novae, and are routinely missed by surveys (e.g. Kasliwal et al. 2011; Shara et al. 2016)—and according to Section 4.1, we might expect such novae to be less likely to form dust. However, a high-cadence survey of novae in the Milky Way using the All-Sky Automated Survey for Supernovae (ASAS-SN; Shappee et al. 2014; Kochanek et al. 2017) finds no such significant population of faint/fast Galactic novae, implying that our samples of novae detected in recent decades are a reasonable representation of the larger, underlying population (Kawash et al. 2021a, 2022). On the other hand, IR

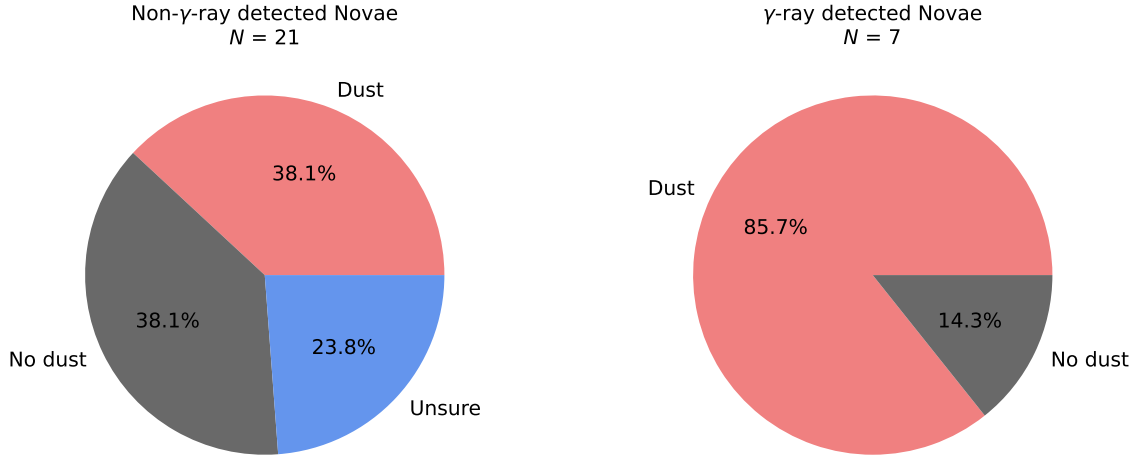


Figure 13. *Left:* a pie chart representing the 21 γ -ray non-detected novae in our sample, divided into non-dust forming (grey), dust forming (light red), and unsure (light blue). *Right:* same as *left* but for the 7 γ -ray detected novae in our sample. There are no ‘unsure’ novae in the γ -ray detected sample.

surveys have demonstrated that there is a significant population of heavily-extinguished novae at the lowest Galactic latitudes (De et al. 2021; Zuckerman et al. 2023), and these novae are systematically missed by optical surveys (Kawash et al. 2021b). These novae are associated with the Milky Way’s thin disk, and therefore may be more likely to occur on relatively massive white dwarfs, yielding relatively short t_2 , small ejecta masses, and high expansion velocities (della Valle et al. 1992; Della Valle & Livio 1998). It is possible, therefore, that a population of fast novae that is relatively unlikely to form dust is currently mostly hidden by the Galactic dusty foreground.

Currently, \lesssim half of Galactic novae are discovered by a patchwork of surveys and efforts (Shafter 2017; De et al. 2021; Kawash et al. 2022; Zuckerman et al. 2023), and only a subset are observed in the IR to enable assessment of their dust formation properties. The next generation of all-sky surveys, including the Legacy Survey of Space and Time (LSST; Ivezić et al. 2019), WINTER, and PRIME, will feature red/near-IR bands capable of penetrating the Galactic dusty foregrounds that currently limit the discovery of Galactic novae (Kawash et al. 2021b). These red/IR bands will also reveal whether individual novae have formed dust, improving estimates of dust formation rates among novae.

4.3 Are γ -ray detected novae more likely to form dust?

Galactic novae are routinely detected in GeV γ -rays by *Fermi*-LAT (Abdo et al. 2010; Ackermann et al. 2014; Cheung et al. 2016; Franckowiak et al. 2018), but the γ -ray properties of novae are diverse, with at least a two orders of magnitude spread in their >100 MeV luminosities (Chomiuk et al. 2021a). This diversity implies there is a range of shock luminosities in novae, which could in turn translate to a diversity in dust formation properties, if dust is formed in radiative shocks (Derdzinski et al. 2017).

In Figure 13, we compare the dust formation statistics of novae that were detected by *Fermi*-LAT (left panel) with a group of novae that were searched in the *Fermi*-LAT data

but did not lead to significant detections (right panel). Some novae in our sample erupted before the launch of *Fermi*, while others were discovered after the launch of *Fermi* but do not have γ -ray analyses published; we do not include these novae in the pie-charts (see Table 1 for references to γ -ray analyses, or lack thereof). The pie-charts are divided into ‘slices’ of our nova dust classes (dust forming, non dust forming, and unsure).

Our results show that among the γ -ray detected novae, 86_{-21}^{+5} per cent of them form dust, while 1 out of 7 (RS Oph) is believed to not form dust in its eruptions (although dust is observed in the symbiotic binary host; Evans et al. 2007). This stands in remarkable contrast with novae that are not detected in γ -rays, where only 38_{-9}^{+11} per cent form dust, while the same fraction do not show features of dust formation. The rest of the non- γ -ray detected novae (24_{-7}^{+11} per cent) are classified as unsure.

Does this mean that γ -ray luminous novae are more likely to form dust? Derdzinski et al. (2017) linked strong γ -ray emitting shocks with dust formation, suggesting that the regions behind radiative shock fronts provide ideal conditions for dust formation. The rapid cooling of the shocked gas and the dense environment allow the dust to efficiently condense while shielding it from the irradiation by the central white dwarf. Our statistics show that there is an obvious correlation between dust formation and γ -ray detection, which is consistent with the theory of Derdzinski et al. (2017). However, it is worth noting that γ -ray non-detections do not necessarily imply the absence of shocks. Novae detected in γ -rays by *Fermi*-LAT tend to be optically bright (brighter than 8 mag in the V -band; Craig et al. 2025, in prep.), implying that these novae are nearby, and suggesting that distance could be more important than γ -ray luminosity in determining if a nova is detected by *Fermi*-LAT. This means that energetic shocks could still be present in novae not detected in γ -rays, if they are distant. The connection between dust formation and shocks in novae could be further tested by comparing γ -ray luminosity (or upper limits therein) with dust formation properties; this will be a subject of investigation in Craig

et al. (2025, in preparation). Increasing the sample of γ -ray detected novae with dedicated optical and IR follow up will also improve our statistics and help us better understand this connection.

4.4 What do the properties of dust formation episodes correlate with?

A correlation between the time-scale on which dust forms and nova speed class (t_2) has been remarked upon for decades (Gallagher 1977; Bode & Evans 1982), finding that the onset of dust formation starts earlier for faster novae. More recently, Shafter et al. (2011a) confirmed a clear correlation between the time for dust to condense (which they take to be the start of the dust dip) and t_2 for a sample of novae in the Milky Way and M31. Shafter et al. (2011a) and Williams (2013) argue that this correlation is a bit unexpected, as the dust condensation time t_{cond} depends on nova luminosity L and ejecta velocity v_{ej} as $t_{\text{cond}} \propto L^{1/2} v_{\text{ej}}^{-1}$ (Evans & Rawlings 2008). Substituting in scalings of L and v_{ej} with t_2 (Warner 2008; including the controversial maximum magnitude–rate of decline relation; Kasliwal et al. 2011; Shafter et al. 2023), they find that t_{cond} should be largely independent of t_2 . Williams (2013) adapts this model to account for the fact that a nova’s spectral energy distribution hardens over the course of its eruption, and find they can explain the correlation.

We revisit this correlation with our data set in Figure 14, where we plot the time elapsed between V_{peak} and the beginning of the optical dip/IR-excess ($t_{\text{dust,start}}$ in Table 1) against t_2 . Consistent with other studies, we find a striking correlation. Overplotted on the data is a unity line, showing where the time of onset of dust formation and t_2 are identical, and we find that the data adhere to it quite closely. Therefore, the correlation between the time of dust onset and t_2 may simply be driven by the fact that the nova declines below 2 mag from peak *because* it forms dust. Take, for example, V357 Mus (Figure 1); its V -band light curve gently and gradually declines from maximum for ~ 3 weeks, before it plummets due to the dust formation episode starting around day 20 (blue bar in Figure 1). The t_2 value for this nova is 23 days, after the onset of dust formation, implying that the dust formation episode played a role in setting t_2 . This effect can lead to some unintuitive results, as in the dusty nova V1280 Sco, which is one of the slowest novae ever observed in terms of its expansion velocities and time for the optical spectrum to go nebular (Naito et al. 2012), but which has a V -band t_2 of just 21.3 days (Hounsell et al. 2010), placing it in the fast nova speed class. This fast t_2 is driven by the fact that V1280 Sco formed dust, and experienced a dramatic optical dust dip, just a few weeks into its massive eruption (Das et al. 2008; Naito et al. 2012; Sakon et al. 2016). While t_2 is sometimes used as a proxy for expansion velocity (e.g., Warner 2008; Shafter et al. 2011b), the fact that it is dust formation that determines t_2 in $\sim 1/3$ of novae undermines this use case. We instead encourage investigators to make more direct measurements of expansion velocity using spectroscopy. Alternatively, if investigators have the goal of using light curve shape to parameterize the properties of the ejecta (i.e., mass, velocity, density), it may be beneficial to use a redder band than V , where dust absorption will have less of an impact.

Does the duration of the dust episode also correlate with

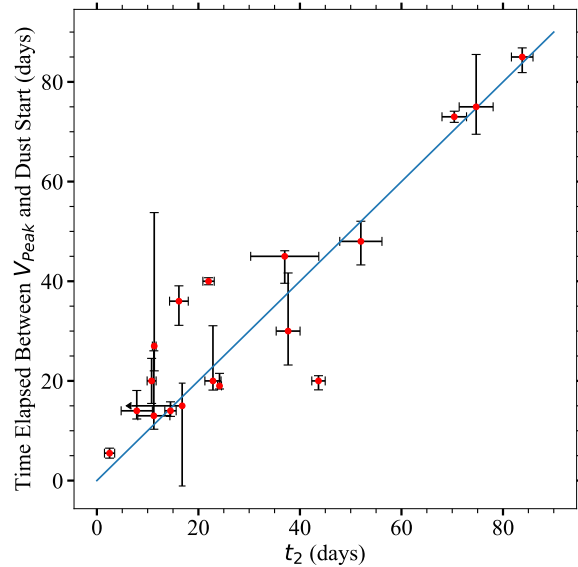


Figure 14. The time elapsed between V_{peak} and the onset of dust formation plotted against t_2 for the dust forming novae in our sample (V5584 Sgr and PR Lup are excluded due to gap in photometric coverage during dust event, N LMC 2009b is excluded due to lack of t_2 data). The blue line is a unity line for which $x = y$.

t_2 ? If the recovery from dust dip is driven by the destruction of dust in the harsh radiation field of the nuclear-burning white dwarf, we might expect slower novae to have longer duration dust events, because their relatively slow/massive ejecta will take longer to unveil the harsh radiation field of the white dwarf. Figure 15 plots Δt_{dust} (the time elapsed between the onset of dust formation and the bottom of the dust event) against t_2 for the dust-forming novae in our sample. Our results show that there is no obvious correlation between these two parameters, with a correlation coefficient of just $r = -0.03$. Apparently, additional factors beyond nova speed class are at work in determining the duration of dust events, or perhaps, as suggested by Shore et al. (2018), the recovery from the dust dip does not require significant destruction of grains, but could just be an effect of the thinning out of the ejecta. We also searched for a correlation between the time of the onset of the dust dip and the duration of the dust dip, and similarly found no correlation.

Strope et al. (2010) claim that the deeper a nova’s dust dip (as observed in their V -band light curves), the later this dust dip will occur. We test this assertion in Figure 16, where on the x -axis we plot $t_{\text{dust,start}}$, and on the y -axis, we plot the change in the V -band brightness over the course of the dust event, ΔV_{dust} . We see no correlation between the parameters, with a correlation coefficient of $r = 0.01$. Take, for example, the deepest dust dip in our sample, V357 Mus with $\Delta V_{\text{dust}} = 10.3$, which begins forming dust after just 20 days. We find a similar lack of correlation when we plot the depth of the dust dip against the duration of the dust dip (e.g., the ordinate of Figure 15), or when we characterize the ‘depth’ of the dust dip as the redward change in the $(V - K)$ colour index over the course of the dust formation episode. We conclude that there is no clear correlation between the depth of a dust dip

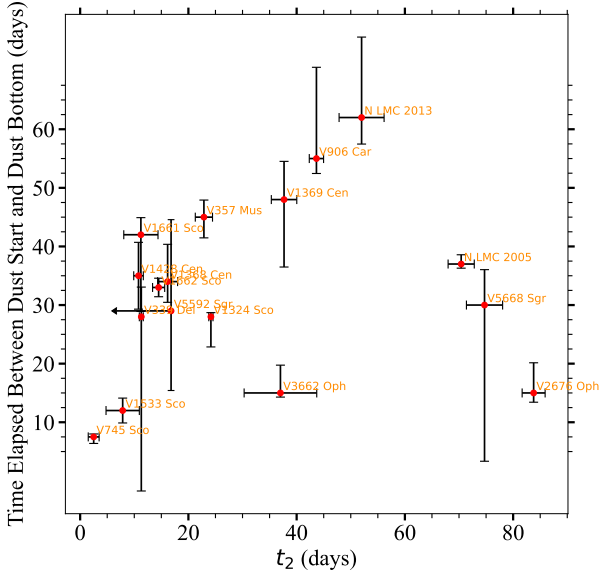


Figure 15. The time elapsed between the onset of dust formation episode and the bottom of the dust event plotted against t_2 for the dust-forming novae in our sample (V475 Sct, V5584 Sgr and PR Lup are excluded due to gap in photometric coverage during dust event, N LMC 2009b is excluded due to lack of t_2 data). The correlation coefficient between the two parameters is $r = -0.03$

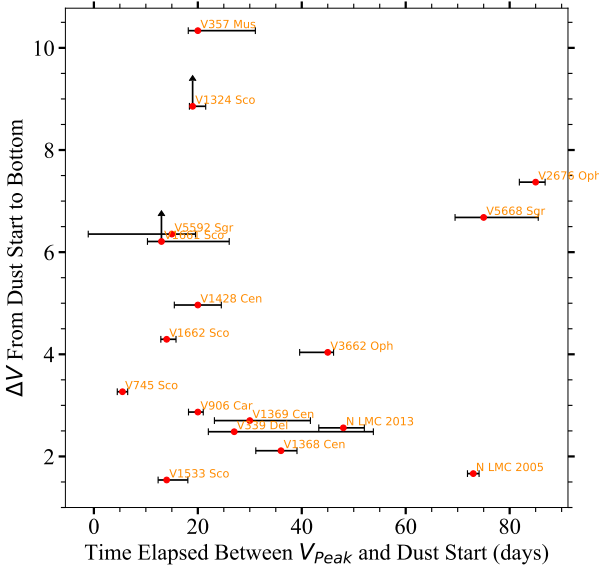


Figure 16. The depth of the V -band dust dip (in magnitudes) plotted against the time lag between optical light curve peak and the onset of dust formation for the dust-forming novae in our sample (V475 Sct, V5584 Sgr and PR Lup are excluded due to gap in photometric coverage during dust event, N LMC 2009b is excluded due to lack of V_{Peak} data.). The correlation coefficient between the two parameters is $r = 0.02$.

and its time-scale. A lack of correlation would be expected if the dust only covers a portion of the nova ejecta, and the depth of the dust dip (and indeed, whether it is an optically thick dust dip or an optically thin IR excess) is primarily determined by inclination and viewing effects, as suggested by [Derdzinski et al. \(2017, e.g., their figure 1\)](#).

5 CONCLUSIONS

We performed a statistical analysis of dust formation in a sample of 40 well-observed novae with extensive optical and IR photometric coverage ([Walter et al. 2012](#)). Our results show that between 50 and 70 per cent of novae form dust (Section 4.2), a fraction substantially higher than previous estimates in the literature (e.g., [Strope et al. 2010](#)). While this fraction holds true for currently discovered Galactic novae, it could be biased if current surveys are systematically missing some sub-populations of Galactic novae. The prevalence of dust formation in novae makes them ideal, nearby laboratories to explore the physics of dust condensation in astrophysical transients.

We propose a simple diagnostic of dust formation in novae: the largest redward change in $(V - K)$ relative to the colour at V -band light curve peak (Figure 8). There is a clear separation between novae that form dust and those that do not, with dust-forming novae showing $\Delta(V - K) > 2.35$. We note that novae with red giant companions present a more complicated picture, and may show $\Delta(V - K) > 2.35$ even if they do not form dust. $(V - J)$ and $(V - H)$ colour indices are also useful for identifying dust formation episodes, but are likely to have higher false positive rates than $(V - K)$ (Section 3.2). Time-domain surveys in IR bands, like WINTER and PRIME, have the potential to find every nova eruption in the Milky Way, and also determine which of them form dust.

By comparing our dust formation statistics with nova speed class (quantified by t_2 , the time for the V -band light curve to decline by two magnitudes from peak), we find that very fast novae ($t_2 \leq 10$ days) are much less likely to form dust than their slower counterparts (Figures 11 and 12). While this trend has been noticed for decades ([Gallagher 1977](#)), our data are the clearest demonstration of the effect to date, with just 17 per cent of very fast novae forming dust, compared with ~ 70 per cent of slower novae with $t_2 = 11 - 80$ days. We do, however, view the subtle, short-lived dust formation episode in the very fast nova V745 Sco as a cautionary tale ([Banerjee et al. 2023b](#)), and encourage the use of IR spectroscopy to identify molecular species like CO (which are tracers of dust), to assess the prevalence of mild dust formation episodes that could be missed by photometry alone (these may be more common in very fast novae).

We also assess whether novae detected in GeV γ -rays by *Fermi*-LAT are more likely to form dust, as might be expected if dust forms in radiative shock fronts ([Derdzinski et al. 2017](#)). We find a signal with 86 per cent of γ -ray detected novae forming dust, vs. just 38 per cent of novae that are not detected by *Fermi* (Figure 13). Future studies should dig deeper into this trend by comparing γ -ray luminosity (or upper limits) with dust formation properties.

We confirm the correlation between t_2 and the time of the onset of dust formation studied by [Shafter et al. \(2011a\)](#) and

Williams et al. (2013, see Figure 14). However, we find that it can simply be explained if $t_2 \approx t_{\text{cond}}$ (the condensation time-scale of dust formation), i.e. the nova is observed to drop 2 magnitudes below light curve maximum *because* it formed dust (Section 4.4). Future work should search for a more physically robust connection between the timescale of dust formation and nova properties like luminosity, ejecta velocity, and eject mass, by comparing e.g., t_{cond} with v_{ej} directly.

How dust forms around explosive transients remains a perplexing puzzle in high-energy astrophysics. This work provides a first step towards a quantitative characterization of dust formation in a population of novae. A second future step would be to collect detailed multi-wavelength observations (e.g., spectroscopy, X-ray observations, etc.) in order to reveal what nova properties dust formation and survival depend upon. In addition, high-resolution imaging has the potential to reveal the locations of dust condensation within the nova ejecta, further testing if dust forms at nova shocks. This work also provides strong motivation for IR transient surveys and follow-up observations, all with the aim of uncovering the mystery of dust production in explosive transients.

ACKNOWLEDGEMENTS

This paper was inspired by conversations with Brian Metzger, Andrea Derdzinski, and Jenő Sokolowski. A.C., E.A., P.C., L.C., and A.S. are grateful for support from NASA grants 80NSSC23K0497, 80NSSC23K1247, and 80NSSC25K7334 and NSF grants AST-2107070 and AST-2205628. E.A. acknowledges support by NASA through the NASA Hubble Fellowship grant HST-HF2-51501.001-A awarded by the Space Telescope Science Institute, which is operated by the Association of Universities for Research in Astronomy, Inc., for NASA, under contract NAS5-26555. This research has used data from the SMARTS 1.3 m, 1.0 m, and 0.9 m telescopes, which are operated as part of the SMARTS Consortium.

DATA AVAILABILITY

The data are available as online material and can be found here:

https://www.dropbox.com/scl/fo/vkkoodp7dtz65jugmrafp/ANUc6HAe8Cm_3-HGykZtg_A?rlkey=k1le8ko4a8xy9ixzjehda9tcq&st=d8rhtnpy&dl=0

REFERENCES

- Abdo A. A., et al., 2010, *Science*, **329**, 817
- Ackermann M., et al., 2014, *Science*, **345**, 554
- Arai A., et al., 2010, *PASJ*, **62**, 1103
- Ashok N. M., Banerjee D. P. K., 2003, *A&A*, **409**, 1007
- Atwood W. B., et al., 2009, *ApJ*, **697**, 1071
- Aydi E., et al., 2019, arXiv e-prints,
- Aydi E., Chomiuk L., Sokolovsky K. V., Steinberg E., 2020a, *Nature Astronomy*, **2**, 697
- Aydi E., et al., 2020b, *ApJ*, **905**, 62
- Babul A.-N., et al., 2022, *MNRAS*, **515**, 3028
- Banerjee D. P. K., Ashok N. M., 2012, *Bulletin of the Astronomical Society of India*, **40**, 243
- Banerjee D. P. K., Srivastava M. K., Ashok N. M., Venkataraman V., 2016, *MNRAS*, **455**, L109
- Banerjee D. P. K., Srivastava M. K., Ashok N. M., Munari U., Hamsch F. J., Righetti G. L., Maitan A., 2018, *MNRAS*, **473**, 1895
- Banerjee D. P. K., Evans A., Woodward C. E., Starrfield S., Su K. Y. L., Ashok N. M., Wagner R. M., 2023a, *ApJ*, **952**, L26
- Banerjee D. P. K., et al., 2023b, *ApJ*, **954**, L16
- Barry R. K., et al., 2008, *ApJ*, **677**, 1253
- Beck H., Gail H. P., Gass H., Sedlmayr E., 1990, *A&A*, **238**, 283
- Bode M. F., Evans A., 1982, *MNRAS*, **200**, 175
- Bode M. F., Evans A., 2008, in *Classical Novae*, 2nd Edition. Edited by M.F. Bode and A. Evans. Cambridge Astrophysics Series, No. 43, Cambridge: Cambridge University Press, 2008..
- Bode M. F., Evans A., Whittet D. C. B., Aitken D. K., Roche P. F., Whitmore B., 1984, *MNRAS*, **207**, 897
- Bode M. F., et al., 2016, *ApJ*, **818**, 145
- Brandi E., Quiroga C., Mikolajewska J., Ferrer O. E., García L. G., 2009, *A&A*, **497**, 815
- Burlak M. A., Esipov V. F., Komissarova G. V., Shenavrin V. I., Taranova O. G., Tatarnikov A. M., Tatarnikova A. A., 2015, *Baltic Astronomy*, **24**, 109
- Cameron E., 2011, *Publications of the Astronomical Society of Australia*, **28**, 128
- Cheung C. C., et al., 2016, *ApJ*, **826**, 142
- Cheung C. C., et al., 2022, *ApJ*, **935**, 44
- Chochol D., et al., 2006, *Chinese Journal of Astronomy and Astrophysics Supplement*, **6**, 137
- Chomiuk L., Metzger B. D., Shen K. J., 2021a, *ARA&A*, **59**, 391
- Chomiuk L., et al., 2021b, *ApJS*, **257**, 49
- Cunningham T., Wolf W. M., Bildsten L., 2015, *ApJ*, **803**, 76
- Darnley M. J., 2021, in *The Golden Age of Cataclysmic Variables and Related Objects* V. p. 44 ([arXiv:1912.13209](https://arxiv.org/abs/1912.13209)), doi:10.22323/1.368.0044
- Darnley M. J., Henze M., 2020, *Advances in Space Research*, **66**, 1147
- Das R. K., Banerjee D. P. K., Ashok N. M., Chesneau O., 2008, *MNRAS*, **391**, 1874
- De K., et al., 2020, *PASP*, **132**, 025001
- De K., et al., 2021, *ApJ*, **912**, 19
- Della Valle M., Izzo L., 2020, *A&ARv*, **28**, 3
- Della Valle M., Livio M., 1998, *ApJ*, **506**, 818
- della Valle M., Bianchini A., Livio M., Orio M., 1992, *A&A*, **266**, 232
- Derdzinski A. M., Metzger B. D., Lazzati D., 2017, *MNRAS*, **469**, 1314
- Ebel D. S., 2000, *J. Geophys. Res.*, **105**, 10363
- Evans A., 1990, in Cassatella A., Viotti R., eds., Vol. 369, IAU Colloq. 122: Physics of Classical Novae. Springer-Verlag, Berlin, Germany; New York, NY, p. 253, doi:10.1007/3-540-53500-4_133
- Evans A., 1997, *Ap&SS*, **251**, 293
- Evans A., 2001, *Ap&SS*, **275**, 131
- Evans A., Gehrz R. D., 2012, *Bulletin of the Astronomical Society of India*, **40**, 213
- Evans E., Rawlings J. M. C., 2008, in *Classical Novae*, 2nd Edition. Edited by M.F. Bode and A. Evans. Cambridge Astrophysics Series, No. 43, Cambridge: Cambridge University Press, 2008.. pp 308–334
- Evans A., et al., 2007, *ApJ*, **671**, L157
- Evans A., et al., 2010, *MNRAS*, **406**, L85
- Evans A., et al., 2017, *MNRAS*, **466**, 4221
- Franckowiak A., Jean P., Wood M., Cheung C. C., Buson S., 2018, *A&A*, **609**, A120
- Gaia Collaboration et al., 2016, *A&A*, **595**, A1
- Gaia Collaboration et al., 2023, *A&A*, **674**, A1
- Gallagher J. S., 1977, *AJ*, **82**, 209

- Gallagher J. S., Anderson C. M., 1976, *ApJ*, **203**, 625
- Gallagher J. S., Starrfield S., 1978, *ARA&A*, **16**, 171
- Gehrz R. D., 1988, *ARA&A*, **26**, 377
- Gehrz R. D., 2002, in Hernanz M., José J., eds, American Institute of Physics Conference Series Vol. 637, Classical Nova Explosions. AIP, pp 198–207, doi:10.1063/1.1518200
- Gehrz R. D., 2008, in Classical Novae, 2nd Edition. Edited by M.F. Bode and A. Evans. Cambridge Astrophysics Series, No. 43, Cambridge: Cambridge University Press, 2008.. pp 167–193
- Gehrz R. D., Truran J. W., Williams R. E., Starrfield S., 1998, *PASP*, **110**, 3
- Gehrz R. D., et al., 2015, *ApJ*, **812**, 132
- Gehrz R. D., et al., 2018, *ApJ*, **858**, 78
- Geisel S. L., Kleinmann D. E., Low F. J., 1970, *ApJ*, **161**, L101
- Gordon A. C., Aydi E., Page K. L., Li K.-L., Chomiuk L., Sokolovsky K. V., Mukai K., Seitz J., 2021, *ApJ*, **910**, 134
- Habtie G. R., Das R., Pandey R., Ashok N. M., Dubovsky P. A., 2024, *MNRAS*, **527**, 1405
- Hamada R., et al., 2024, The Astronomer’s Telegram, **16824**, 1
- Helton L. A., et al., 2012, *ApJ*, **755**, 37
- Hounsell R., et al., 2010, *ApJ*, **724**, 480
- Ivezić Ž., et al., 2019, *ApJ*, **873**, 111
- José J., Hernanz M., 2007, *Meteoritics & Planetary Science*, **42**, 1135
- Joshi V., Banerjee D. P. K., Ashok N. M., Venkataraman V., Walter F. M., 2015, *MNRAS*, **452**, 3696
- Kasliwal M. M., Cenko S. B., Kulkarni S. R., Ofek E. O., Quimby R., Rau A., 2011, *ApJ*, **735**, 94
- Kawash A., et al., 2021a, *ApJ*, **910**, 120
- Kawash A., et al., 2021b, *ApJ*, **922**, 25
- Kawash A., et al., 2022, *ApJ*, **937**, 64
- Kloppenborg B. K., 2023, Observations from the AAVSO International Database, <https://www.aavso.org>. AAVSO
- Kochanek C. S., et al., 2017, *PASP*, **129**, 104502
- Lau R. M., et al., 2022, *Nature Astronomy*, **6**, 1308
- Liller W., Monard L. A. G., 2009, IAU Circ., **9042**, 1
- Liller W., Heathcote B., di Scala G., Allen W., 2007, *JAAVSO*, **35**, 359
- Linford J. D., et al., 2017, *ApJ*, **842**, 73
- Lourie N. P., et al., 2020, in Evans C. J., Bryant J. J., Motohara K., eds, Society of Photo-Optical Instrumentation Engineers (SPIE) Conference Series Vol. 11447, Ground-based and Airborne Instrumentation for Astronomy VIII. p. 114479K ([arXiv:2102.01109](https://arxiv.org/abs/2102.01109)), doi:10.1117/12.2561210
- Metzger B. D., Hascoët R., Vurm I., Beloborodov A. M., Chomiuk L., Sokoloski J. L., Nelson T., 2014, *MNRAS*, **442**, 713
- Metzger B. D., Finzell T., Vurm I., Hascoët R., Beloborodov A. M., Chomiuk L., 2015, *MNRAS*, **450**, 2739
- Morgan G. E., Ringwald F. A., Buil C., Garrett M., 2005, *PASP*, **117**, 938
- Mróz P., et al., 2016, *ApJS*, **222**, 9
- Mukai K., Orio M., Della Valle M., 2008, *ApJ*, **677**, 1248
- Munari U., Banerjee D. P. K., 2018, *MNRAS*, **475**, 508
- Munari U., Hamsch F. J., Frigo A., 2017, *MNRAS*, **469**, 4341
- Naito H., et al., 2012, *A&A*, **543**, A86
- Ney E. P., Hatfield B. F., 1978, *ApJ*, **219**, L111
- Nishimura H., Nakano S., 2012, Central Bureau Electronic Telegrams, **3166**, 1
- O’Brien T. J., Bode M. F., 2008, in Classical Novae, 2nd Edition. Edited by M.F. Bode and A. Evans. Cambridge Astrophysics Series, No. 43, Cambridge: Cambridge University Press, 2008.. pp 285–306
- Page K. L., Beardmore A. P., Osborne J. P., 2020, *Advances in Space Research*, **66**, 1169
- Payne-Gaposchkin C. H. P., 1957, The galactic novae. Amsterdam, North-Holland Pub. Co.; New York, Interscience Publishers
- Amsterdam, North-Holland Pub. Co.; New York, Interscience Publishers
- Rawlings J. M. C., 1988, *MNRAS*, **232**, 507
- Rawlings J. M. C., Williams D. A., 1989, *MNRAS*, **240**, 729
- Sakon I., et al., 2016, *ApJ*, **817**, 145
- Samus N. N., Kazarovets E., 2004, IAU Circ., **8445**, 2
- Schaefer B. E., 2010, *ApJS*, **187**, 275
- Schaefer B. E., 2018, *MNRAS*, **481**, 3033
- Schaefer B. E., 2022, *MNRAS*, **517**, 6150
- Schlafly E. F., Finkbeiner D. P., 2011, *ApJ*, **737**, 103
- Schwarz G. J., et al., 2011, *ApJS*, **197**, 31
- Schwarz G. J., et al., 2015, *AJ*, **149**, 95
- Shafter A. W., 2017, *ApJ*, **834**, 196
- Shafter A. W., Bode M. F., Darnley M. J., Misselt K. A., Rubin M., Hornoch K., 2011a, *ApJ*, **727**, 50
- Shafter A. W., et al., 2011b, *ApJ*, **734**, 12
- Shafter A. W., Clark J. G., Hornoch K., 2023, *Research Notes of the American Astronomical Society*, **7**, 191
- Shappee B. J., et al., 2014, *ApJ*, **788**, 48
- Shara M. M., 1981, *ApJ*, **243**, 926
- Shara M. M., et al., 2016, *ApJS*, **227**, 1
- Shore S. N., Kuin N. P., Mason E., De Gennaro Aquino I., 2018, *A&A*, **619**, A104
- Sokolovsky K. V., et al., 2020, *MNRAS*, **497**, 2569
- Sokolovsky K. V., et al., 2022, *MNRAS*, **514**, 2239
- Sokolovsky K. V., et al., 2023, *MNRAS*, **521**, 5453
- Srivastava M. K., Banerjee D. P. K., Ashok N. M., Venkataraman V., Sand D., Diamond T., 2016, *MNRAS*, **462**, 2074
- Strope R. J., Schaefer B. E., Henden A. A., 2010, *AJ*, **140**, 34
- Szkody P., Dyck H. M., Capps R. W., Becklin E. E., Cruikshank D. P., 1979, *AJ*, **84**, 1359
- Usov V. V., 1991, *MNRAS*, **252**, 49
- van den Bergh S., Younger P. F., 1987, *A&AS*, **70**, 125
- Walter F. M., Battisti A., Towers S. E., Bond H. E., Stringfellow G. S., 2012, *PASP*, **124**, 1057
- Warner B., 2008, in Classical Novae, 2nd Edition. Edited by M.F. Bode and A. Evans. Cambridge Astrophysics Series, No. 43, Cambridge: Cambridge University Press, 2008.. pp 16–33
- Wee J., et al., 2020, *ApJ*, **899**, 162
- Williams R. E., 1990, in Cassatella A., Viotti R., eds, , Vol. 369, IAU Colloq. 122: Physics of Classical Novae. Springer-Verlag, Berlin, Germany; New York, NY, p. 215, doi:10.1007/3-540-53500-4_12910.1007/3-540-53500-4
- Williams R. E., 1994, *ApJ*, **426**, 279
- Williams R., 2013, *AJ*, **146**, 55
- Williams S. C., Bode M. F., Darnley M. J., Evans A., Zubko V., Shafter A. W., 2013, *ApJ*, **777**, L32
- Wolf W. M., Bildsten L., Brooks J., Paxton B., 2013, *ApJ*, **777**, 136
- Woodward C. E., Banerjee D. P. K., Evans A., Wagner R. M., Starrfield S., 2021, The Astronomer’s Telegram, **14741**, 1
- Woudt P. A., et al., 2009, *ApJ*, **706**, 738
- Wyrzykowski L., Udalski A., Kozłowski S., Skowron J., 2013, The Astronomer’s Telegram, **5491**, 1
- Yama H., et al., 2023, *Journal of Astronomical Instrumentation*, **12**, 2350004
- Yaron O., Prialnik D., Shara M. M., Kovetz A., 2005, *ApJ*, **623**, 398
- Zuckerman L., De K., Eilers A.-C., Meisner A. M., Panagiotou C., 2023, *MNRAS*, **523**, 3555

APPENDIX A: FULL SAMPLE OF NOVA LIGHT CURVES

For convenience, we include individual light curves and colour curves for all 40 novae in our sample (Table 1). The top panel of each plot includes the K -band light curve in black and the V -band light curve in green. The bottom panel shows the $(V - K)$ colour as a function of time. These values are observed, not intrinsic, and therefore not corrected for extinction. The captions include the names of the novae and their assigned dust classification. For ‘Dust Dip’ and ‘IR Excess’ novae, the dotted blue vertical line represents an estimate of the start time of the dust event, with the blue shaded region extending from the last $(V - K)$ data point before it to the first $(V - K)$ data point after it. The vertical dotted red line represents an estimate of the ‘bottom’ of the dust event, when the nova is most red as measured by $(V - K)$. The red shaded region extends from the last $(V - K)$ data point before the dotted red line to the first $(V - K)$ data point after it. These shaded regions are shown with the intent of providing a more objective representation of our confidence in the precision of our estimates, and are accounted for as error bars on the time-scales of dust formation in Figures 14–16.

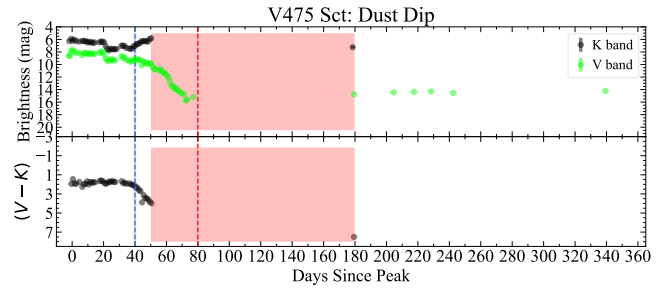


Figure A.1. The V and K light curves (*Top*) and $(V - K)$ colour curve (*Bottom*) of nova V475 Sct, which we classify as ‘Dust Dip’. The blue vertical bar denotes the earliest feature attributable to the dust event (in this case, a rise in the K -band light curve), while the red vertical bar marks the ‘bottom’ of the dust dip (the point immediately after the $(V - K)$ colour appears to have finished the large redward shift caused by dust formation). The width of the bars is set by the cadence of the photometry at these times. We hypothesize that the ‘bottom’ of the dust dip in V475 Sct occurs near the beginning of the solar conjunction based on optical light and colour curves from Chochol et al. (2006).

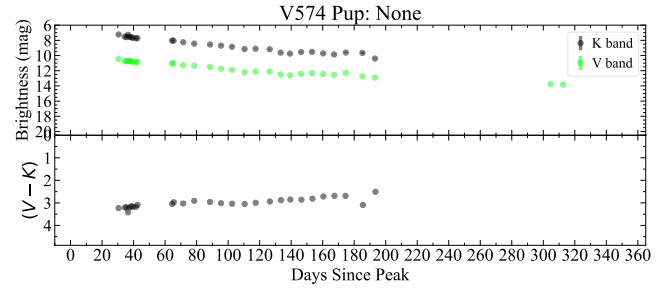


Figure A.2. Same as Figure A.1 but for nova V574 Pup, which we classify as ‘None’.

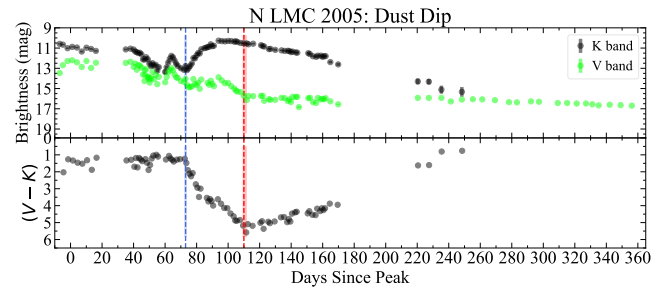


Figure A.3. Same as Figure A.1 but for nova N LMC 2005, which we classify as ‘Dust Dip’.

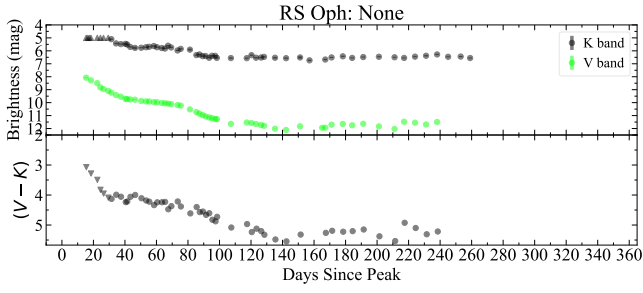


Figure A.4. Same as Figure A.1 but for nova RS Oph (2006), which we classify as ‘None’.

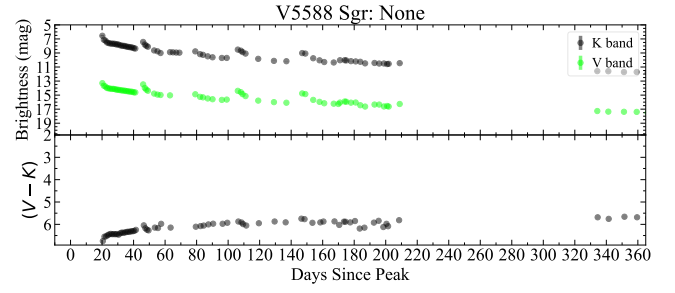


Figure A.8. Same as Figure A.1 but for nova V5588 Sgr, which we classify as ‘None’.

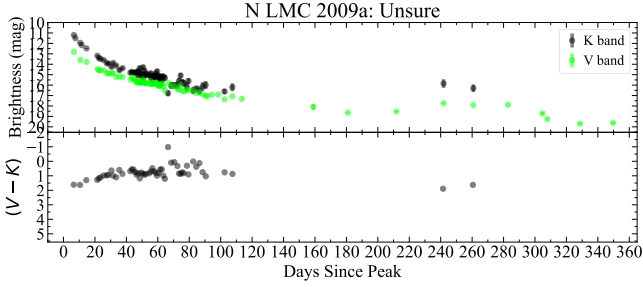


Figure A.5. Same as Figure A.1 but for nova N LMC 2009a, which we classify as ‘Unsure’.

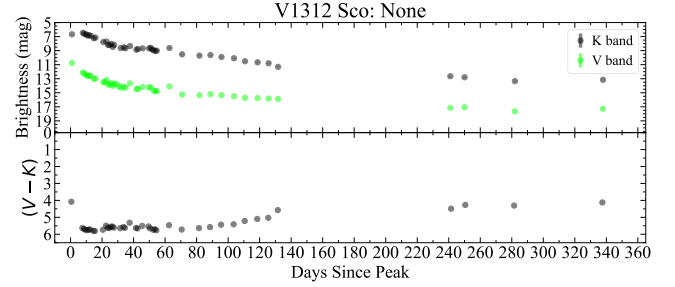


Figure A.9. Same as Figure A.1 but for nova V1312 Sco, which we classify as ‘None’.

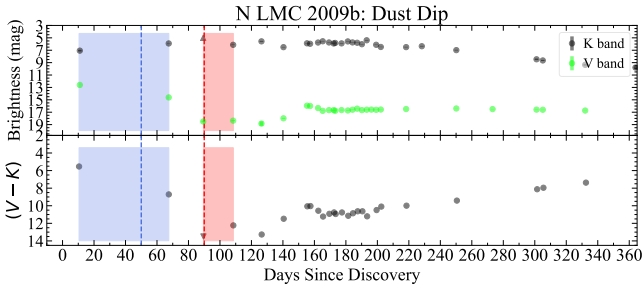


Figure A.6. Same as Figure A.1 but for nova N LMC 2009b, which we classify as ‘Dust Dip’.

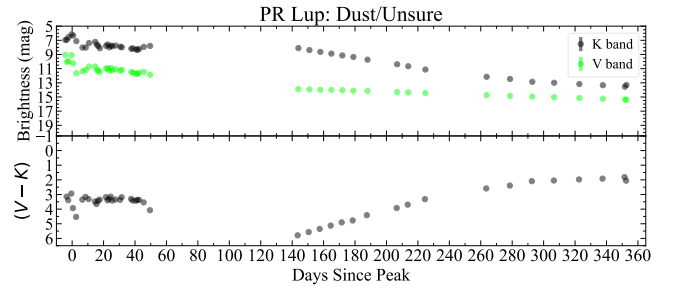


Figure A.10. Same as Figure A.1 but for nova PR Lup, which we classify as ‘Dust/Unsure’.

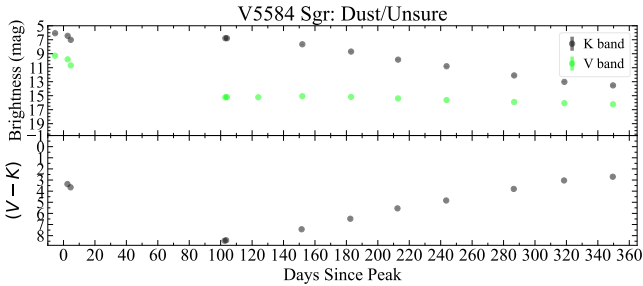


Figure A.7. Same as Figure A.1 but for nova V5584 Sgr, which we classify as ‘Dust Dip’.

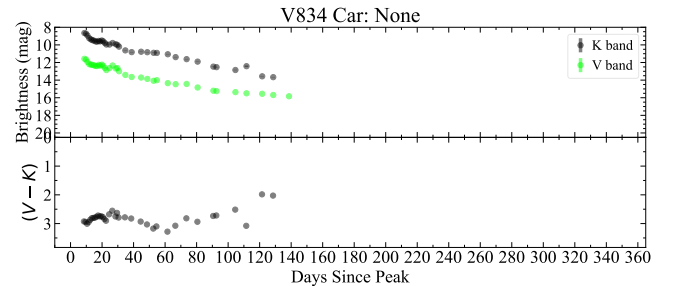


Figure A.11. Same as Figure A.1 but for nova V834 Car, which we classify as ‘None’.

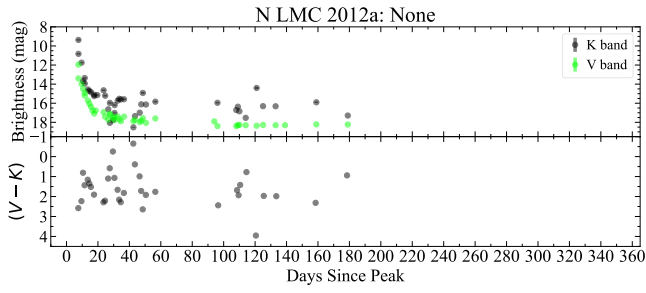


Figure A.12. Same as Figure A.1 but for nova N LMC 2012a, which we classify as ‘None’.

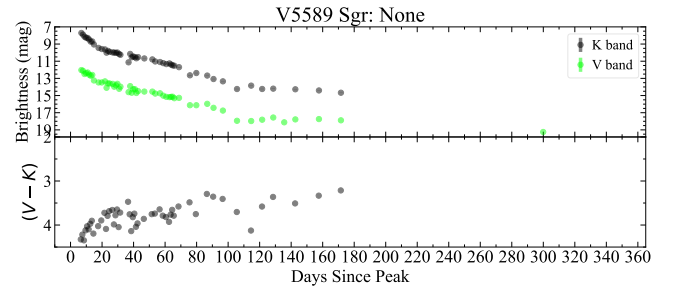


Figure A.16. Same as Figure A.1 but for nova V5589 Sgr, which we classify as ‘None’.

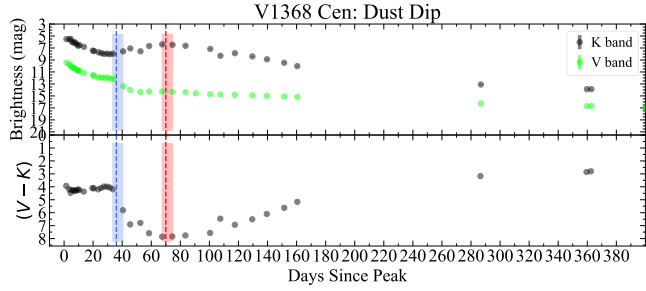


Figure A.13. Same as Figure A.1 but for nova V1368 Cen, which we classify as ‘Dust Dip’.

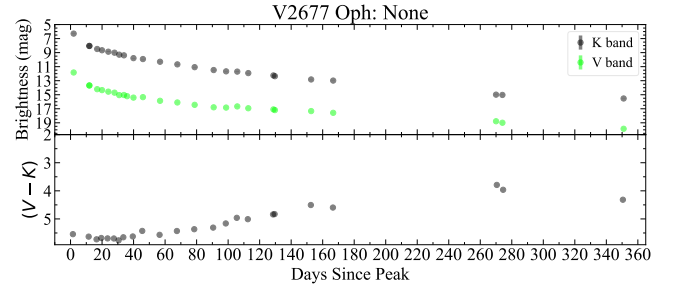


Figure A.17. Same as Figure A.1 but for nova V2677 Oph, which we classify as ‘None’.

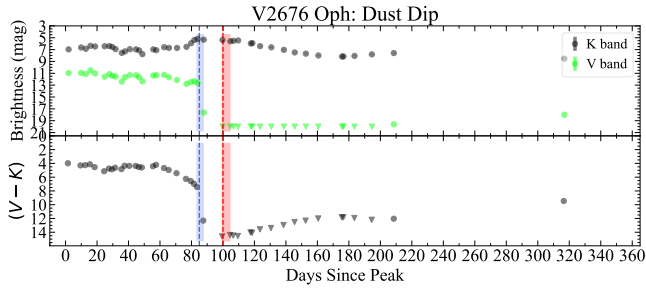


Figure A.14. Same as Figure A.1 but for nova V2676 Oph, which we classify as ‘Dust Dip’.

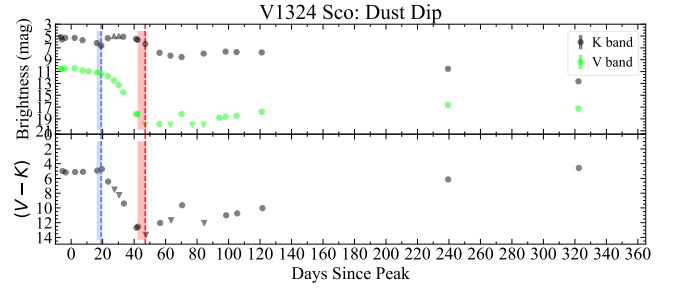


Figure A.18. Same as Figure A.1 but for nova V1324 Sco, which we classify as ‘Dust Dip’.

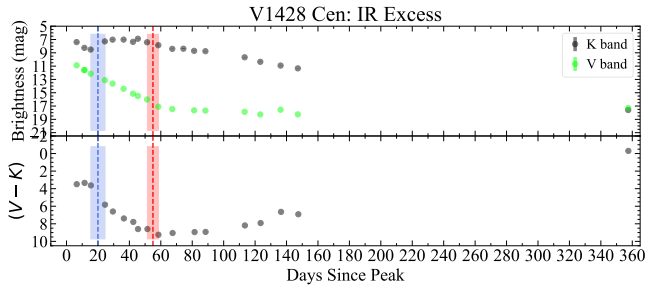


Figure A.15. Same as Figure A.1 but for nova V1428 Cen, which we classify as ‘IR Excess’.

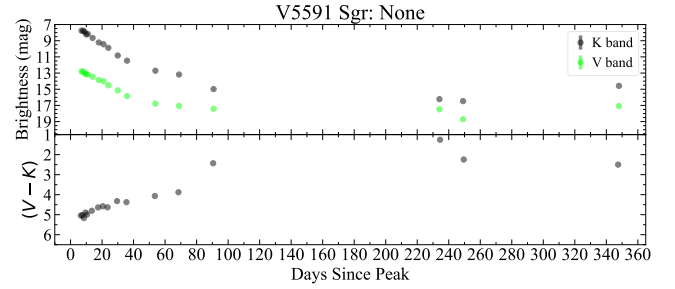


Figure A.19. Same as Figure A.1 but for nova V5591 Sgr, which we classify as ‘None’.

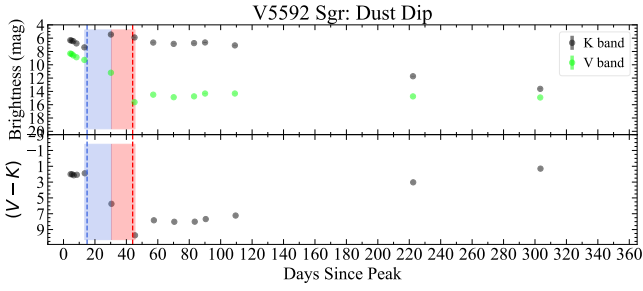


Figure A.20. Same as Figure A.1 but for nova V5592 Sgr, which we classify as ‘Dust Dip’.

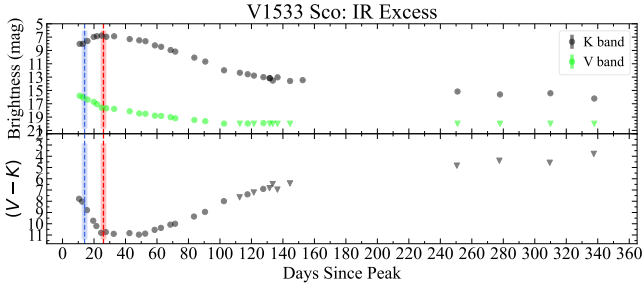


Figure A.21. Same as Figure A.1 but for nova V1533 Sco, which we classify as ‘IR Excess’.

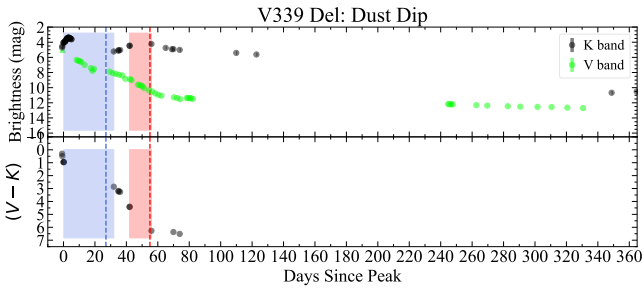


Figure A.22. Same as Figure A.1 but for nova V339 Del, which we classify as ‘Dust Dip’. [Gehrz et al. \(2015\)](#) shows a V -band light curve for V339 Del that has measurements out to day ~ 180 , in which the V -band curve starts to flatten between days 60-80, past which point it shows no appreciable dimming. As the K -band light curve does not continue to brighten past day ~ 55 , the nova likely continues to slowly get bluer over time, so we mark the dust event ‘bottom’ at day ~ 55 .

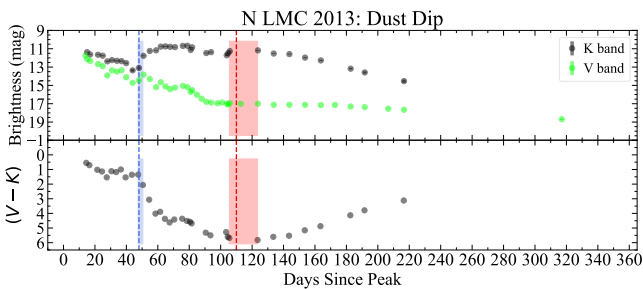


Figure A.23. Same as Figure A.1 but for nova N LMC 2013, which we classify as ‘Dust Dip’.

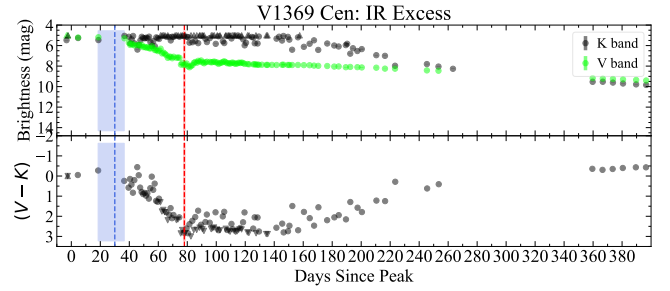


Figure A.24. Same as Figure A.1 but for nova V1369 Cen, which we classify as ‘IR Excess’. Because the first measurement in both the K -band and V -band is saturated, we have used the first V -band measurement after peak as our ‘ V peak in SMARTS Data’ for figures 8, 9, and 10. The two measurements are both close to peak (< 10 days), so this decision should not significantly affect results.

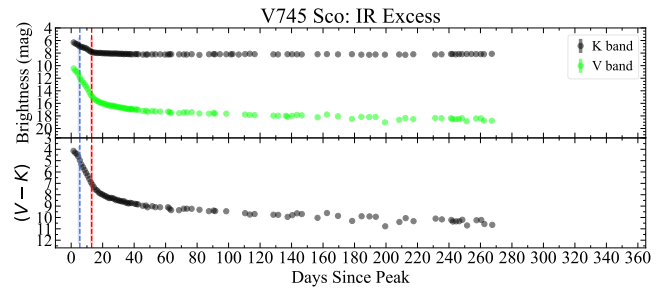


Figure A.25. Same as Figure A.1 but for nova V745 Sco (2014), which we classify as ‘IR Excess’.

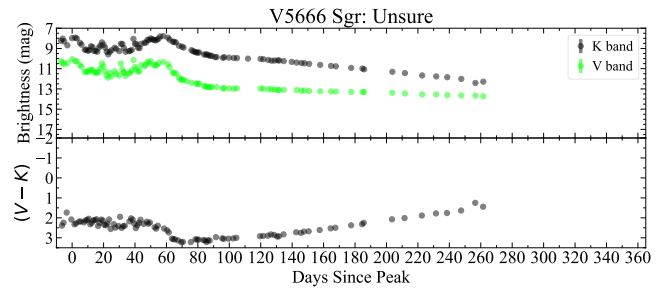


Figure A.26. Same as Figure A.1 but for nova V5666 Sgr, which we classify as ‘Unsure’.

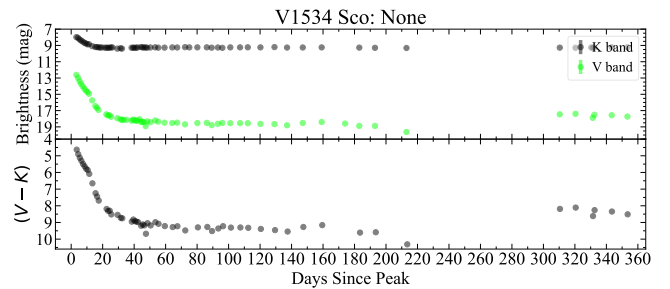


Figure A.27. Same as Figure A.1 but for nova V1534 Sco, which we classify as ‘None’.

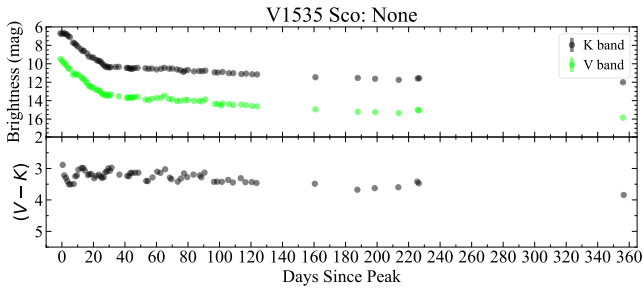


Figure A.28. Same as Figure A.1 but for nova V1535 Sco, which we classify as ‘None’.

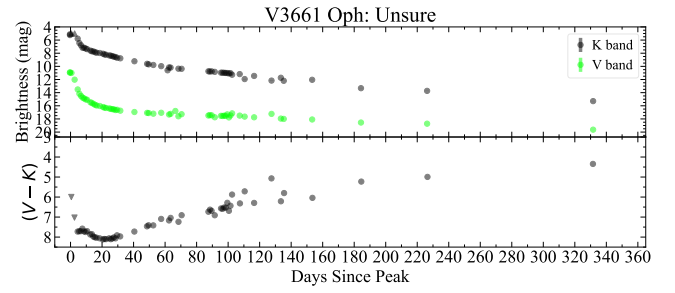


Figure A.32. Same as Figure A.1 but for nova V3661 Oph, which we classify as ‘Unsure’.

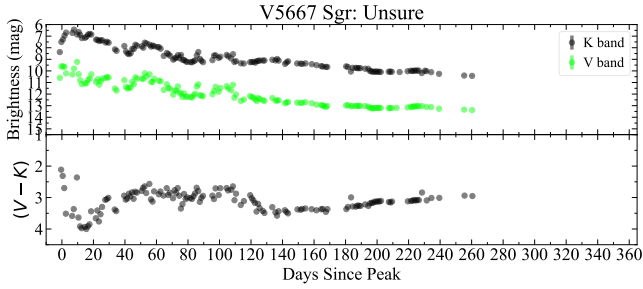


Figure A.29. Same as Figure A.1 but for nova V5667 Sgr, which we classify as ‘Unsure’.

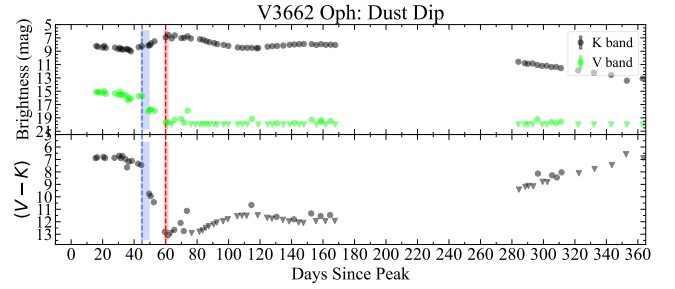


Figure A.33. Same as Figure A.1 but for nova V3662 Oph, which we classify as ‘Dust Dip’.

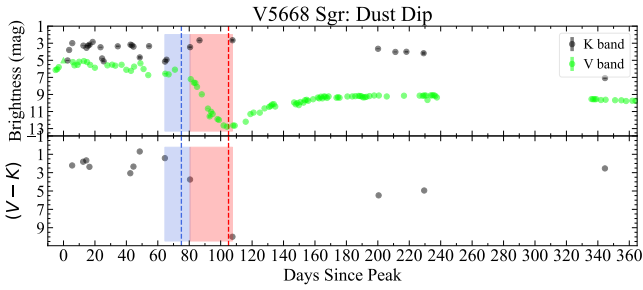


Figure A.30. Same as Figure A.1 but for nova V5668 Sgr, which we classify as ‘Dust Dip’.

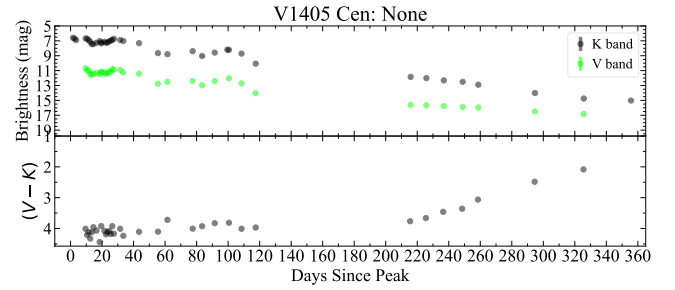


Figure A.34. Same as Figure A.1 but for nova V1405 Cen, which we classify as ‘None’.

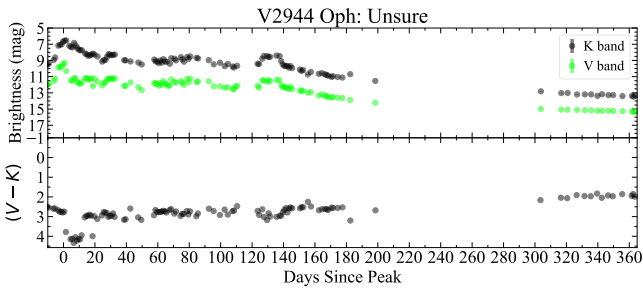


Figure A.31. Same as Figure A.1 but for nova V2944 Oph, which we classify as ‘Unsure’.

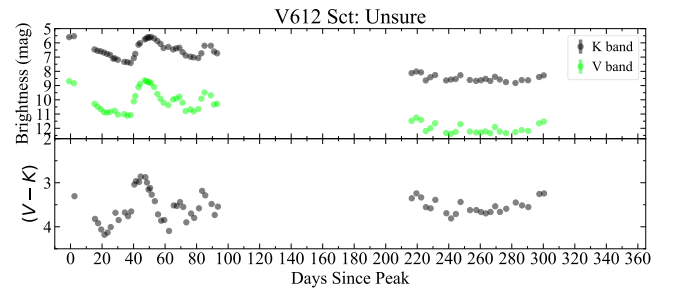


Figure A.35. Same as Figure A.1 but for nova V612 Sct, which we classify as ‘Unsure’.

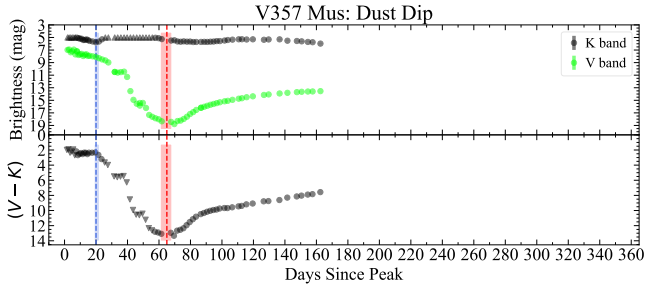


Figure A.36. Same as Figure A.1 but for nova V357 Mus, which we classify as ‘Dust Dip’.

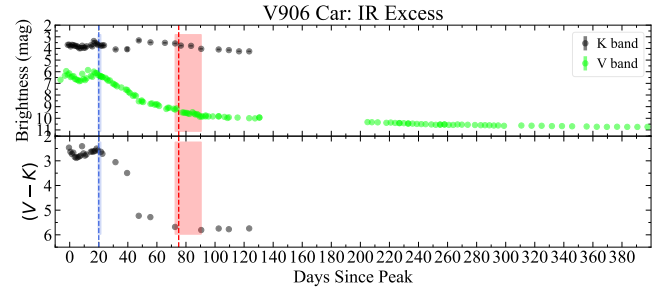


Figure A.40. Same as Figure A.1 but for nova V906 Car, which we classify as ‘IR Excess’.

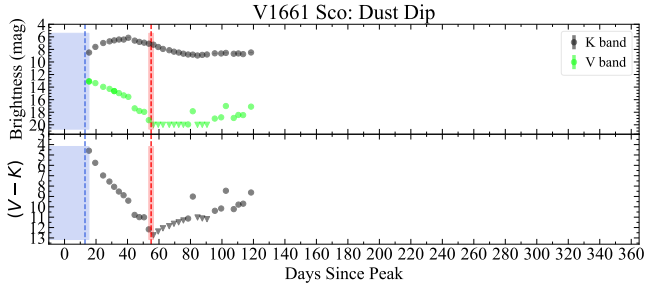


Figure A.37. Same as Figure A.1 but for nova V1661 Sco, which we classify as ‘Dust Dip’.

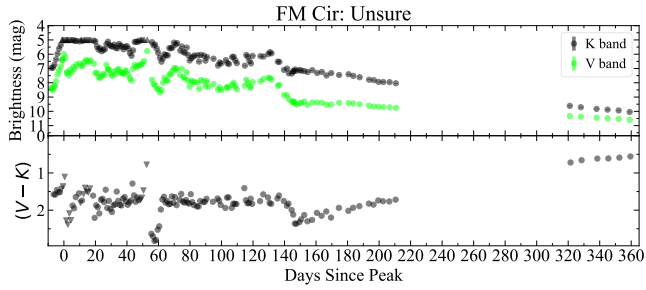


Figure A.38. Same as Figure A.1 but for nova FM Cir, which we classify as ‘Unsure’.

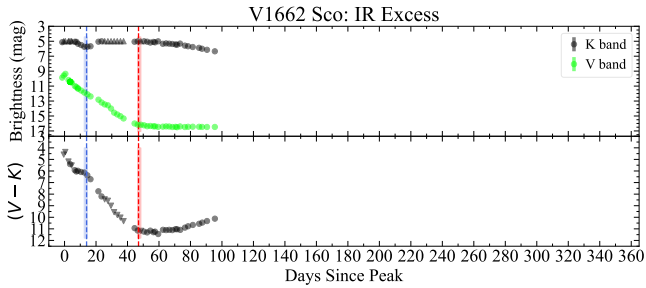


Figure A.39. Same as Figure A.1 but for nova V1662 Sco, which we classify as ‘IR Excess’.

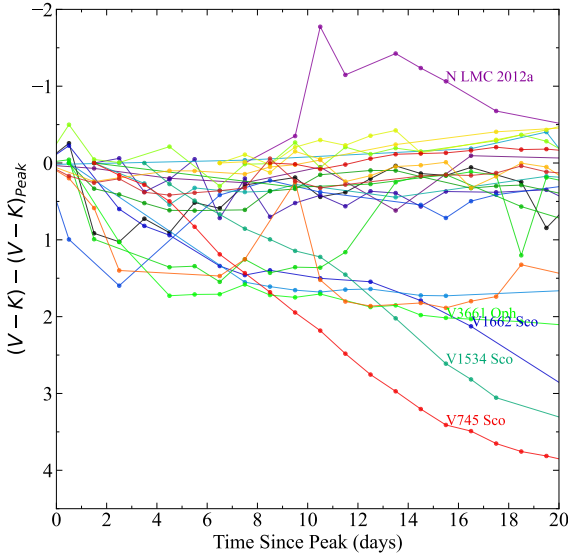


Figure B.1. The evolution of $V - K$ colour for 20 days following V -band peak. Includes light curves with at least 2 measurements between t_{peak} and 10 days after peak, and at least 2 measurements between 10 and 20 days after peak.

APPENDIX B: EVOLUTION OF OPTICAL-IR COLOURS AROUND LIGHT CURVE MAXIMUM

In Section 3, we suggest using the colour change from nova peak as a diagnostic of dust formation. In practice, the cadence of photometry can be limited, and V and/or K may not be measured right at V -band peak. Here we assess how much $(V - K)$ changes around peak, in order to recommend a reasonable time window over which $(V - K)_{peak}$ can be measured.

We track the evolution of the $(V - K)$ colours around the V -band light curve peak, to see how the colours vary with time. The colour evolution for the first 20 days of available SMARTS data is shown in Figure B.1, specifically showing the change in $(V - K)$ since the nova peak. The majority of novae show relatively flat colour curves over this period of time, with their $(V - K)$ reddening slightly from peak but staying within ~ 0.5 mag of $(V - K)_{peak}$ out to 20 days. For the first \sim week of eruption, the colour curves are clustered relatively closely in most novae. Later, the spread in the colour curves increases. The baseline plotted here is too short to capture much of the dust formation in this sample, but it does capture dust formation for those novae that form dust quickly. Three of the novae (V745 Sco, V1534 Sco, and V1662 Sco) redden sufficiently to meet our colour cutoff of $(V - K) - (V - K)_{peak} > 2.35$ on this time-scale. With that said, V745 Sco and V1534 Sco have red giant companions, so in those cases the colour change does not necessarily indicate dust formation. N LMC 2012a shows somewhat uncommon evolution in $(V - K)$, growing significantly bluer after the peak. Otherwise, all of the novae in our sample either retain constant colours compared to the peak, or become redder over time.

A different time baseline is displayed in Figure B.2, with

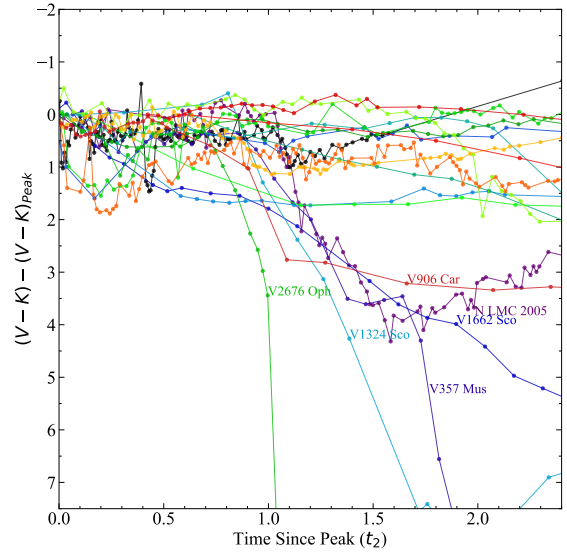


Figure B.2. The evolution of $(V - K)$ colour as a function of time in units of t_2 . Again, light curves with at least 2 measurements between t_{peak} and 10 days after peak, and at least 2 measurements between 10 and 20 days after peak, are included.

the time provided in units of t_2 . While for most novae the time baseline is longer than in Figure B.1, for a few faster novae, $2.4 t_2$ (the upper limit on the x-axis) is less than the 20 days displayed in Figure B.1. Again, we see the colour curves are clustered between $(V - K) - (V - K)_{peak} \approx 0 - 1$ for times earlier than $1 t_2$. At later times, there is far more spread in the colour curves, primarily driven by dust formation. We conclude that a $(V - K)$ colour measured before t_2 can reasonably be used to estimate the colour at peak, with a typical uncertainty of ± 0.5 mag.

APPENDIX C: INTRINSIC OPTICAL-IR COLOURS OF NOVAE AT LIGHT CURVE MAXIMUM

If a nova is not observed at peak, but later optical/IR photometry is obtained and an estimate of the foreground extinction can be made, it is still possible to use the diagnostics suggested in Section 3 to assess whether the nova formed dust. Here we estimate reddening-corrected colours of novae at peak to enable this use case.

Determining intrinsic colours around peak requires estimates of the interstellar reddening towards each nova. This is only available for a small subset of the novae in our sample. For the purpose of measuring colours, we avoid using extinctions measured using the nova's colour in other bands, to avoid potential biases/circular logic. In the spirit of a recent study of optical colours of novae (Craig et al. 2024, submitted), our $E(B - V)$ measurements mostly consist of spectroscopic measurements using Diffuse Interstellar Bands (DIBs), or 3D dust maps when Gaia DR3 parallaxes are available and have errors less than 30 per cent of the parallax (Gaia Collaboration et al. 2016, 2023; Schaefer 2018, 2022). DIB based

measurements are available for some of the novae in our sample in Craig et. al. (2024, submitted). For novae in the LMC, we use the 2D dust maps of Schlafly & Finkbeiner (2011), which should be a reasonable extinction estimate towards the LMC.

Figure C.1 plots the reddening corrected $(V - K)_0$ colours around V -band peak. Based on the sample that we have extinctions for, the average colour at peak is $\langle (V - K) \rangle_{0, \text{peak}} = 1.1$ based on a sample of 9 novae. The $(V - K)$ colours show significantly more variability compared to the colours in optical bands, with a standard deviation of 0.8 mag around peak. The colours near peak in $(B - V)_0$, for comparison, typically vary by ~ 0.3 magnitudes, and even less around t_2 (van den Bergh & Younger 1987; Schaefer 2022, Craig et al. 2024, submitted). At later times, there is a great deal of spread in $(V - K)_0$, likely caused by dust formation in some novae causing large amounts of reddening (some novae can get redder by more than 5 mag). The variability at peak is unlikely to be caused by dust formation in the nova, and likely is a combination of intrinsic variations in the $(V - K)_0$ colours of novae and the uncertainty in determining the interstellar reddening towards these novae.

The $(V - J)_0$ and $(V - H)_0$ colours have also been calculated at the optical peak for this sample. As with the $(V - K)_0$ colours, this is across our sample with extinction measurements and non-saturated SMARTS photometry near the peak. We find that $\langle (V - J) \rangle_{0, \text{peak}} = 0.8$ based on 10 novae, with a standard deviation of 0.6. The standard deviation here is large compared to optical colours, but small compared to $(V - K)_0$. The distribution for $(V - H)_0$ is similar, with $\langle V - H \rangle_{0, \text{peak}} = 0.7$ and a standard deviation of 0.6, based on 9 novae.

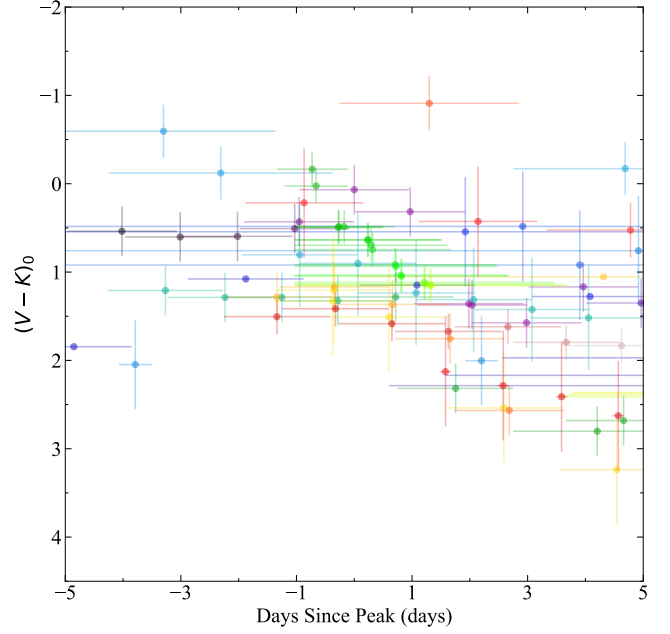


Figure C.1. $(V - K)_0$ colour around peak, corrected for extinction, as a function of time from peak. Vertical error bars are dominated by errors in extinction. Horizontal error bars include uncertainty in t_{peak} and the time difference between the V - and K -band measurements.